Technical Report Documentation Page

1. Report No.	2. Government Accession No.	3. Recipient's Catalog No.
DOT/FAA/ES-83/3		

4. Title and Subtitle
The IF-77 Electromagnetic Wave Propagation Model

5. Report Date
September 1983

6. Performing Organization Code

8. Performing Organization Report No.

7. Author(s)
G. D. Gierhart and M. E. Johnson

9. Performing Organization Name and Address
U.S. Dept. of Commerce
National Telecommunications & Information Administration
Institute for Telecommunication Sciences ITS.S3
325 Broadway Boulder, CO 80303

10. Work Unit No. (TRAIS)

11. Contract or Grant No.
DTFA01-82-Y-10539

13. Type of Report and Period Covered
Final

12. Sponsoring Agency Name and Address
U.S. Dept. of Transportation
Federal Aviation Administration
Systems Engineering Service
Washington, D. C. 20591

14. Sponsoring Agency Code
AES-520

15. Supplementary Notes
FAA Frequency Engineering Branch, AES-520

16. Abstract
This report provides a description of the computational details in the IF-77 (ITS-FAA-1977) radio wave propagation model. The IF-77 model is useful in estimating service coverage for radio systems operating in the 0.1 to 20 GHz frequency range. It is applicable to many air/air, air/ground, air/satellite, ground/ground, and ground/satellite systems. Irregular terrain and propagation beyond the line-of-sight range are considered in the model. However, the terrain feature is keyed to the lower (or facility) antenna and the radio horizon for the upper (or aircraft) antenna is (1) determined from the facility horizon obstacle (common horizon) or (2) taken as the smooth earth radio horizon when a common horizon is negated by the earth's bulge. Previous publications concerning IF-77 include (1) an applications guide for computer programs that use IF-77, (2) an extensive comparison of predictions made using IF-77 with measured data, and (3) an atlas of propagation curves applicable to aeronautical systems. Details concerning the computer programs are not included in this report.

17. Key words
air/air, air/ground; earth/satellite, propagation model, protection ratio, transmission loss

18. Distribution Statement
This document is available to the U. S. public through the National Technical Information Service, Springfield, VA 22161

19. Security Classif. (of this report)	20. Security Classif. (of this page)	21. No. of Pages	22. Price
UNCLASSIFIED	UNCLASSIFIED	89	

English/Metric Conversion Factors

Length

From \ To	Cm	m	Km	in	ft	s mi	nmi
Cm	1	0.01	$1x10^{-5}$	0.3937	0.0328	$6.21x10^{-6}$	$5.39x10^{-6}$
m	100	1	0.001	39.37	3.281	0.0006	0.0005
Km	100,000	1000	1	39370	3281	0.6214	0.5395
in	2.540	0.0254	$2.54x10^{-5}$	1	0.0833	$1.58x10^{-5}$	$1.37x10^{-5}$
ft	30.48	0.3048	$3.05x10^{-4}$	12	1	$1.89x10^{-4}$	$1.64x10^{-4}$
S mi	160,900	1609	1.609	63360	5280	1	0.8688
nmi	185,200	1852	1.852	72930	6076	1.151	1

Area

From \ To	Cm^2	m^2	Km^2	in^2	ft^2	S mi^2	nmi^2
Cm^2	1	0.0001	$1x10^{-10}$	0.1550	0.0011	$3.86x10^{-11}$	$5.11x10^{-11}$
m^2	10,000	1	$1x10^{-6}$	1550	10.76	$3.86x10^{-7}$	$5.11x10^{-7}$
Km^2	$1x10^{10}$	$1x10^{6}$	1	$1.55x10^{9}$	$1.08x10^{7}$	0.3861	0.2914
in^2	6.452	0.0006	$6.45x10^{-10}$	1	0.0069	$2.49x10^{-10}$	$1.88x10^{-10}$
ft^2	929.0	0.0929	$9.29x10^{-8}$	144	1	$3.59x10^{-8}$	$2.71x10^{-8}$
S mi^2	$2.59x10^{10}$	$2.59x10^{6}$	2.590	$4.01x10^{9}$	$2.79x10^{7}$	1	0.7548
nmi^2	$3.43x10^{10}$	$3.43x10^{6}$	3.432	$5.31x10^{9}$	$3.70x10^{7}$	1.325	1

Volume

From \ To	Cm^3	Liter	m^3	in^3	ft^3	yd^3	fl oz	fl pt	fl qt	gal
Cm^3	1	0.001	$1x10^{-6}$	0.0610	$3.53x10^{-5}$	$1.31x10^{-6}$	0.0338	0.0021	0.0010	0.0002
liter	1000	1	0.001	61.02	0.0353	0.0013	33.81	2.113	1.057	0.2642
m^3	$1x10^{6}$	1000	1	61,000	35.31	1.308	33,800	2113	1057	264.2
in^3	16.39	0.0163	$1.64x10^{-5}$	1	0.0006	$2.14x10^{-5}$	0.5541	0.0346	2113	0.0043
ft^3	28,300	28.32	0.0283	1728	1	0.0370	957.5	59.84	0.0173	7.481
yd^3	765,000	764.5	0.7646	46700	27	1	25900	1616	807.9	202.0
fl oz	29.57	0.2957	$2.96x10^{-5}$	1.805	0.0010	$3.87x10^{-5}$	1	0.0625	0.0312	0.0078
fl pt	473.2	0.4732	0.0005	28.88	0.0167	0.0006	16	1	0.5000	0.1250
fl qt	946.3	0.9463	0.0009	57.75	0.0334	0.0012	32	2	1	0.2500
gal	3785	3.785	0.0038	231.0	0.1337	0.0050	128	8	4	1

Mass

From \ To	g	Kg	oz	lb	ton
g	1	0.001	0.0353	0.0022	$1.10x10^{-6}$
Kg	1000	1	35.27	2.205	0.0011
oz	28.35	0.0283	1	0.0625	$3.12x10^{-5}$
lb	453.6	0.4536	16	1	0.0005
ton	907,000	907.2	32,000	2000	1

Temperature

$$^{0}C = 9/5\ (^{0}F - 32)$$

$$^{0}F = 5/9\ (^{0}C) + 32$$

English/Metric Conversion Factors

Length

From \ To	Cm	m	Km	in	ft	s mi	nmi
Cm	1	0.01	$1x10^{-5}$	0.3937	0.0328	$6.21x10^{-6}$	$5.39x10^{-6}$
m	100	1	0.001	39.37	3.281	0.0006	0.0005
Km	100,000	1000	1	39370	3281	0.6214	0.5395
in	2.540	0.0254	$2.54x10^{-5}$	1	0.0833	$1.58x10^{-5}$	$1.37x10^{-5}$
ft	30.48	0.3048	$3.05x10^{-4}$	12	1	$1.89x10^{-4}$	$1.64x10^{-4}$
S mi	160,900	1609	1.609	63360	5280	1	0.8688
nmi	185,200	1852	1.852	72930	6076	1.151	1

Area

From \ To	Cm^2	m^2	Km^2	in^2	ft^2	S mi^2	nmi^2
Cm^2	1	0.0001	$1x10^{-10}$	0.1550	0.0011	$3.86x10^{-11}$	$5.11x10^{-11}$
m^2	10,000	1	$1x10^{-6}$	1550	10.76	$3.86x10^{-7}$	$5.11x10^{-7}$
Km^2	$1x10^{10}$	$1x10^{6}$	1	$1.55x10^{9}$	$1.08x10^{7}$	0.3861	0.2914
in^2	6.452	0.0006	$6.45x10^{-10}$	1	0.0069	$2.49x10^{-10}$	$1.88x10^{-10}$
ft^2	929.0	0.0929	$9.29x10^{-8}$	144	1	$3.59x10^{-8}$	$2.71x10^{-8}$
S mi^2	$2.59x10^{10}$	$2.59x10^{6}$	2.590	$4.01x10^{9}$	$2.79x10^{7}$	1	0.7548
nmi^2	$3.43x10^{10}$	$3.43x10^{6}$	3.432	$5.31x10^{9}$	$3.70x10^{7}$	1.325	1

Volume

From \ To	Cm^3	Liter	m^3	in^3	ft^3	yd^3	fl oz	fl pt	fl qt	gal
Cm^3	1	0.001	$1x10^{-6}$	0.0610	$3.53x10^{-5}$	$1.31x10^{-6}$	0.0338	0.0021	0.0010	0.0002
liter	1000	1	0.001	61.02	0.0353	0.0013	33.81	2.113	1.057	0.2642
m^3	$1x10^{6}$	1000	1	61,000	35.31	1.308	33,800	2113	1057	264.2
in^3	16.39	0.0163	$1.64x10^{-5}$	1	0.0006	$2.14x10^{-5}$	0.5541	0.0346	2113	0.0043
ft^3	28,300	28.32	0.0283	1728	1	0.0370	957.5	59.84	0.0173	7.481
yd^3	765,000	764.5	0.7646	46700	27	1	25900	1616	807.9	202.0
fl oz	29.57	0.2957	$2.96x10^{-5}$	1.805	0.0010	$3.87x10^{-5}$	1	0.0625	0.0312	0.0078
fl pt	473.2	0.4732	0.0005	28.88	0.0167	0.0006	16	1	0.5000	0.1250
fl qt	946.3	0.9463	0.0009	57.75	0.0334	0.0012	32	2	1	0.2500
gal	3785	3.785	0.0038	231.0	0.1337	0.0050	128	8	4	1

Mass

From \ To	g	Kg	oz	lb	ton
g	1	0.001	0.0353	0.0022	$1.10x10^{-6}$
Kg	1000	1	35.27	2.205	0.0011
oz	28.35	0.0283	1	0.0625	$3.12x10^{-5}$
lb	453.6	0.4536	16	1	0.0005
ton	907,000	907.2	32,000	2000	1

Temperature

$$^{0}C = 9/5\ (^{0}F - 32)$$

$$^{0}F = 5/9\ (^{0}C) + 32$$

LIST OF FIGURES

LIST OF FIGURES

where it is in kilometers. Braces are used around parameter dimensions when particular units are called for or when a potential dimension difficulty exists. A list of symbols is provided in the appendix.

2. PROPAGATION MODEL

The ITS-77 propagation model is applicable to air/ground, air/air, ground/satellite, and air/satellite paths. It can also be used for ground/ground paths that are line-of-sight or smooth earth. Model applications are restricted to telecommunication systems operating at radio frequencies from about 0.1 to 20 GHz with antenna heights greater than 0.5 tn. In addition, radio-horizon elevations must be less than the elevation of the higher antenna. The radio horizon for the higher antenna is taken either as a common horizon with the lower antenna or as a smooth earth horizon with the same elevation as the lower antenna effective reflecting plane (Sec. 3.3).

At 0.1 to 20 GHz, propagation of radio energy is affected by the lower, nonionized atmosphere (troposphere), specifically by variations in the refractive index of the atmosphere [1, 2, 3, 4, 6, 9, 18, 23, 30, 33, 34]. Atmospheric absorption and attenuation or scattering due to rain become important at SHF [23, Ch. 8; 28; 34, Ch. 31]. The terrain along and in the vicinity of the great circle path between transmitter and receiver also plays an important part. In this frequency range, time and space variations of received signal and interference ratios lend themselves readily to statistical description [18, 25, 27, 32, 34, Sec. 10].

Conceptually, the model is very similar to the Longley-Rice [26] propagation model for propagation over irregular terrain, particularly in that attenuation versus distance curves calculated for the line-of-sight (Sec. 5), diffraction (Sec. 4), and scatter (Sec. 6) regions are blended together to obtain values in transition regions. In addition, the Longley-Rice relationships involving the terrain parameter Δh are used to estimate radio-horizon parameters when such information is not available from facility siting data (Sec. 3.2). The model includes allowance for:

1. Average ray bending (Sec. 3).
2. Horizon effects (Sec. 3).
3. Long-term power fading (Sec. 10.1).
4. Antenna pattern (elevation only) at each terminal (Sec. 5.2.4).
5. Surface reflection multipath (Sec. 10.2).

6. Tropospheric multipath (Sec. 10.3).

7. Atmospheric absorption (Sec. 9).

8. Ionospheric scintillations (Sec. 10.5).

9. Rain attenuation (Sec. 10.4).

10. Sea state (Sec. 5.2.2).

11. A divergence factor (Sec. 5.2.1).

12. Very high antennas (Sec. 8).

13. Antenna tracking options (Sec. 5.2.4).

Computer programs that utilize ITS-77 calculate transmission loss, power available, power density, and/or a desired-to-undesired signal ratio. These parameters are discussed in Sections 2.1 through 2.4. A computational flow chart is provided in Section 2.1 for transmission loss.

2.1 Transmission Loss

Transmission loss has been defined as the ratio (usually expressed in decibels) of power radiated to the power that would be available at the receiving antenna terminals if there were no circuit losses other than those associated with the radiation resistance of the receiving antenna [34, Sec. 2]. Transmission loss levels, L(q), that are not exceeded during a fraction of the time q (or 100 q percent of the time) are calculated from:

$$L(q) = L_b(0.5) + L_{gp} - G_{ET} - G_{ER} - Y_\Sigma(q) \quad \text{dB} \qquad (1)$$

where $L_b(0.5)$ is the median basic transmission loss [32, Sec. 10.4], L_{gp} is the path antenna gain-loss [26, Sec. 1-31], G_{ET} and G_{ER} are free-space antenna gains for the transmitter and receiver at the appropriate elevation angle, respectively, and $Y_\Sigma(q)$ is the total variability from equation 229 of Section 10; i.e.: (229).

Median basic transmission loss, $L_b(0.5)$, is calculated from:

$$L_b(0.5) = L_{br} + A_\gamma + A, \quad \text{dB} \qquad (2)$$

where L_{br} is a calculated reference level of basic transmission loss, A_γ, is a conditional adjustment factor, and A, is atmospheric absorption from (228) of Section 9. The factor, A_γ, from (243) of Section 10.1, is used to prevent available signal

powers from exceeding levels expected for free-space propagation by an unrealistic amount when the variability about $L_b(0.5)$ is large and $L_b(0.5)$ is near its free-space level.

Free-space basic transmission loss, L_{bf}, from (226) of Section 8, terrain attenuation, AT, from (221) of Section 7, and a variability adjustment term, $V_e(0.5)$, from (240) of Section 10.1, are used to determine L_{br}; i.e.:

$$L_{br} = L_{bf} + A_T - V_e(0.5) \quad \text{dB} \tag{3}$$

The value for L_{gp} in (1) is taken as 0 dB in the IF-77 model. This is valid when (a) transmitting and receiving antennas have the same polarization and (b) the maximum antenna gain is less than 50 dB [26, Sec. 1-3].

Values of GET and G_{ER} for (1) are obtained from GET = $G_T + G_{NT}$ and $G_{ER} = G_R + G_{NR}$; i.e.:

$$G_{ET,R} = G_{T,R} + G_{NT,R} \quad \text{dBi} \tag{4}$$

where $G_{T,R}$ is the transmitter or receiver main-beam maximum free space antenna gain in decibels greater than isotropic (dBi), and $G_{NT,R}$ is a normalized transmitting or receiving antenna gain in decibels greater than maximum gain that gives relative gain for the appropriate elevation angle, These gains are all model input parameters. Normalized vertical (elevation) antenna patterns are used to define $G_{NT,R}$ so that gain values can be obtained for elevation angles at which the maximum gain is not appropriate. The calculation of these elevation angles is discussed in Section 5.2.4. Horizontal antenna patterns are not usually considered part of the IF-77 model, but an allowance for them can be made by adjusting $G_{T,R}$ values. However, horizontal patterns have been included in one computer program called TWIRL [20, p. 61].

Variabilities associated with long-term power fading, surface reflection multipath, tropospheric multipath, rain attenuation, and ionospheric scintillation are included in $Y_\varepsilon(q)$ of (1). These are all discussed in Section 10. Since the adjustment terms associated with long-term power fading are included in the calculation of $L_b(0.5)$, $Y_\varepsilon(0.5) = 0$.

A computational flow diagram for L(q) is provided in Figure 1. Although only those equations discussed in this section are included in the diagram, section references are provided for the other calculations involved. Horizon and diffraction

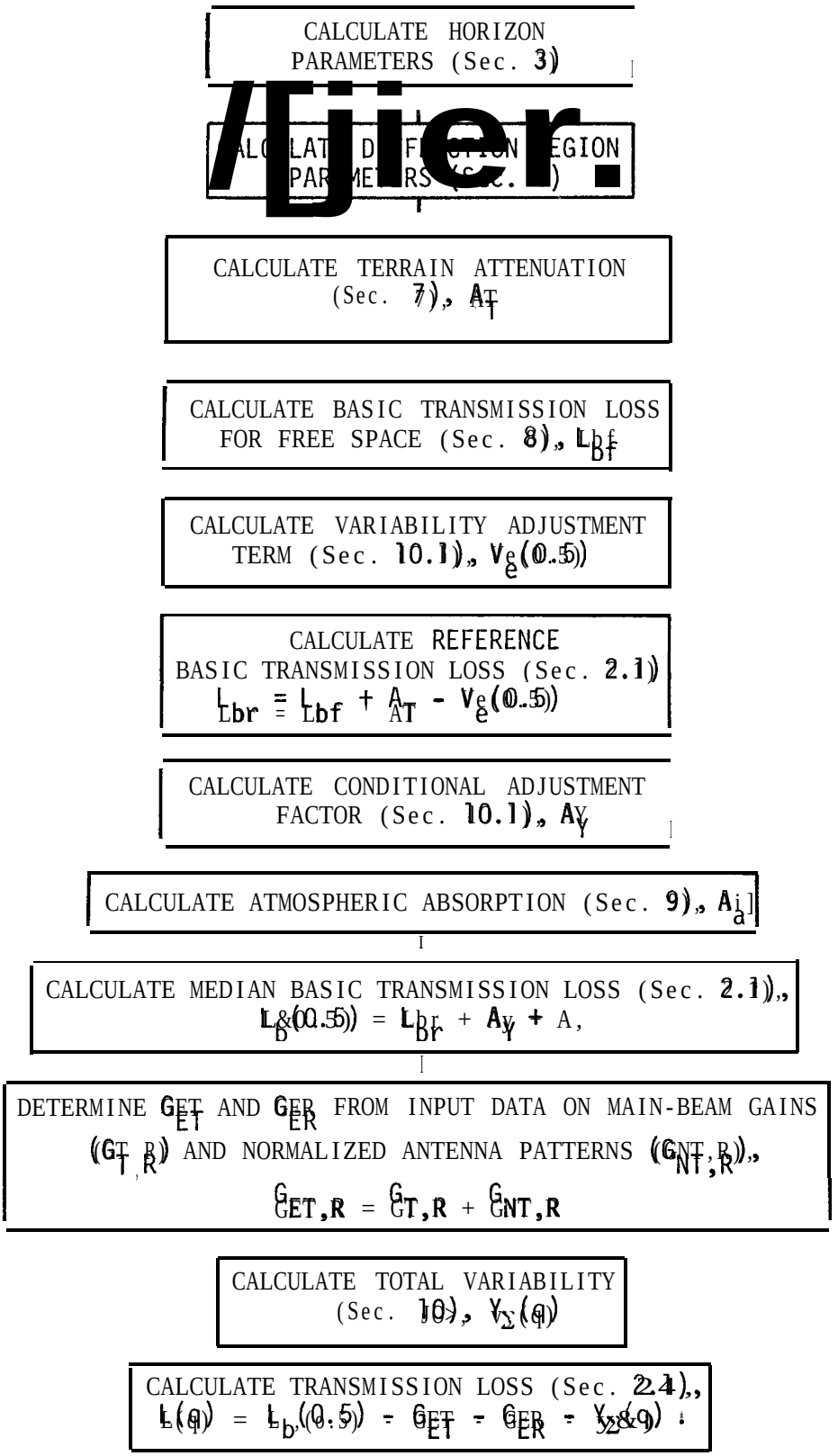

FIGURE 1. COMPUTATIONAL FLOW DIAGRAM FOR L(q).

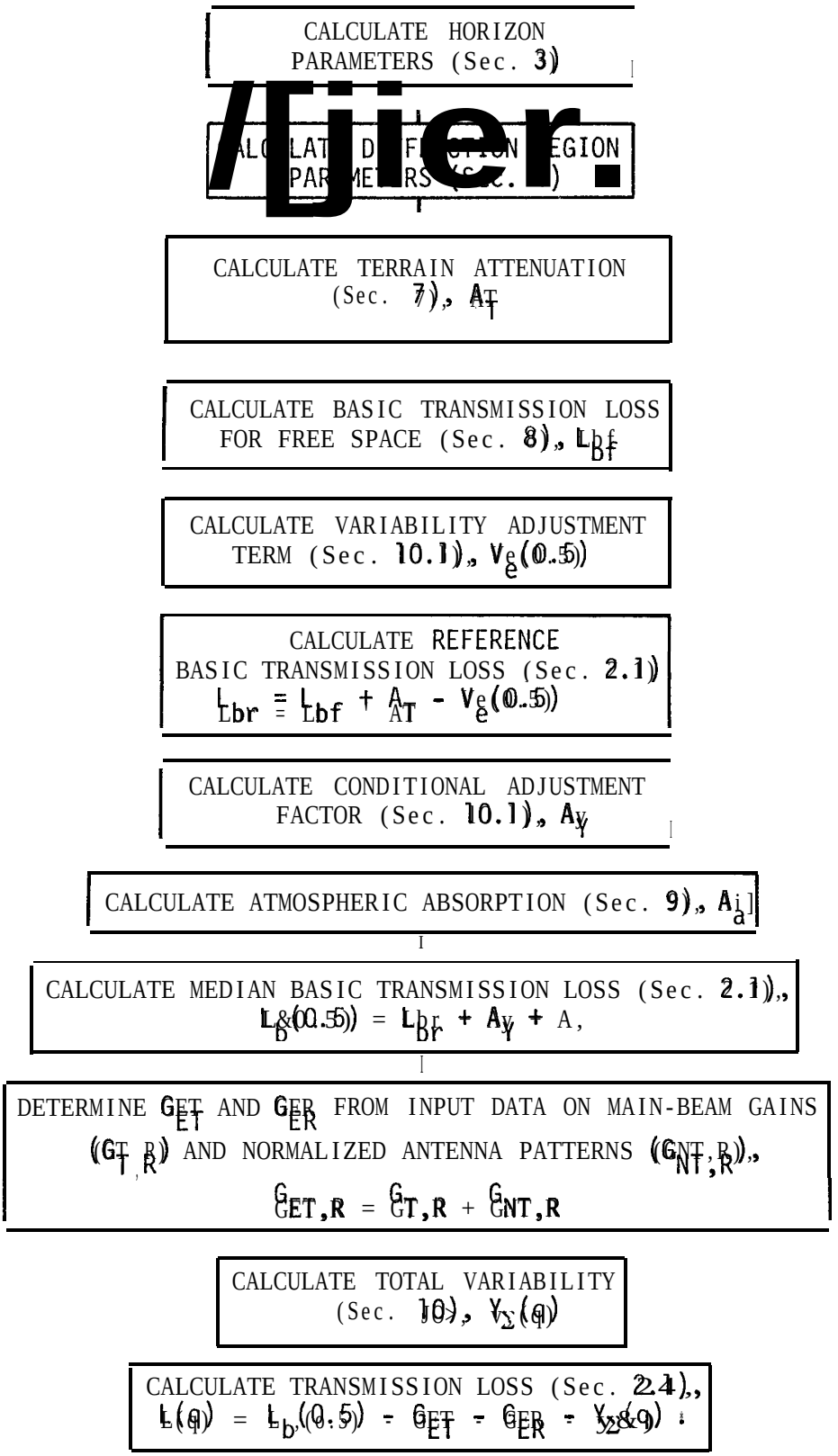

FIGURE 1. COMPUTATIONAL FLOW DIAGRAM FOR L(q).

Values of A_I are determined from:

$$A_I = 10 \log (\lambda_m^2/4\pi) \quad \text{dB-sq m} \tag{9}$$

where λ_m is the wavelength in meters (33, Sec. 4.11). For a frequency of f [MHz]:

$$\lambda_m = 299.7925/f \quad \text{m} \tag{10a}$$

$$A = \lambda_m/1000 \quad \text{km} \tag{10b}$$

2.4 Desired-to-Undesired Signal Ratio

Desired-to-undesired signal ratios that are available for at least a fraction time q, D/U(q) dB, at the terminals of a lossless receiving antenna are calculated using [11, Sec. 3]:

$$D/U(q) = D/U(0.5) + Y_{DU}(q) \quad \text{dB} \tag{11}$$

The median value of D/U(0.5) and the variability $Y_{DU}(q)$ of D/U are calculated as:

$$D/U(0.5) = [P_a(0.5)]_{Desired} - [P_a(0.5)]_{Undesired} \tag{12}$$

$$Y_{DU}(q) = \begin{cases} - \sqrt{[Y_\Sigma(q)]^2_{Desired} + [Y_\Sigma(1-q)]^2_{Undesired}} & \text{dB} \\ \quad \text{for } q \geq 0.5 \\ + \quad \text{otherwise} \end{cases} \tag{13}$$

Values of $P_a(0.5)$ are calculated from (5) where $Y_\Sigma(0.5) = 0$ by using parameters appropriate for either the desired or undesired facility. Applicable variabilities are calculated using the methods described in Section 10. Note that $Y_{DU}(q)$ requires the undesired facility Y_Σ for (1 - q); e.g.:

$$Y_{DU}(0.8) = - \sqrt{[Y_\Sigma(0.8)]^2_{Desired} + [Y_\Sigma(0.2)]^2_{Undesired}}$$

3. HORIZON GEOMETRY

Calculations associated with horizon geometry involve the use of the effective earth radius concept in which ray bending caused by refraction within the troposphere is simplified by using straight rays above an earth with an effective radius that is selected to compensate for the ray bending [3, Sec. 3.6; 30]. The effective earth earth radius, a, is calculated [34, Sec. 4] using the minimum monthly mean surface refractivity referred to mean sea level, N_0, and the height of the effective reflection surface above mean sea level (msl), h_r; i.e.:

$$N_s = \text{greater of} \left\{ \begin{array}{c} N_0 \exp(-0.1057\, h_r) \\ \text{or} \\ 200 \end{array} \right\} \text{ N-units} \quad (14)$$

$$a_0 = 6370 \text{ km} \quad (15)$$

$$a = a_0 [1 - 0.04665 \exp(0.005577\, N_s)]^{-1} \text{ km} \quad (16)$$

Here N_s is surface refractivity at the effective reflecting surface, and a_0 is the actual earth radius to three significant figures. Both N_0 [20, p. 74, p. 94] and h_r [20, p. 83] are model input parameters.

When high (> 10 km) antennas are involved, geometry based solely on the effective radius method may overestimate ray bending so that smooth earth horizon distances become excessive [31]. This difficulty is compensated for in IF-77 by the use of ray tracing in the determination of some key parameters such as effective terminal altitudes (Sec. 3.1), smooth earth horizon distances (Sec. 3.1), and effective distance (Sec. 10.1). In IF-77, ray tracing is performed through an exponential atmosphere [3, equations 3.43, 3.44, 3.40] in which the refractivity, N, varies with height above msl, h, as:

$$N = N_s \exp[-C_e (h - h_r)] \text{ N-units} \quad (17)$$

where

$$C_e = \log_e \left(\frac{N_s}{N_s + \Delta N} \right) \quad (18)$$

and

$$\Delta N = -7.32 \exp(0.005577\, N_s) \text{ N-units/km} \quad (19)$$

3. HORIZON GEOMETRY

Calculations associated with horizon geometry involve the use of the effective earth radius concept in which ray bending caused by refraction within the troposphere is simplified by using straight rays above an earth with an effective radius that is selected to compensate for the ray bending [3, Sec. 3.6; 30]. The effective earth earth radius, a, is calculated [34, Sec. 4] using the minimum monthly mean surface refractivity referred to mean sea level, N_0, and the height of the effective reflection surface above mean sea level (msl), h_r; i.e.:

$$N_s = \text{greater of} \left\{ \begin{array}{c} N_0 \exp(-0.1057\, h_r) \\ \text{or} \\ 200 \end{array} \right\} \text{ N-units} \quad (14)$$

$$a_0 = 6370 \text{ km} \quad (15)$$

$$a = a_0 [1 - 0.04665 \exp(0.005577\, N_s)]^{-1} \text{ km} \quad (16)$$

Here N_s is surface refractivity at the effective reflecting surface, and a_0 is the actual earth radius to three significant figures. Both N_0 [20, p. 74, p. 94] and h_r [20, p. 83] are model input parameters.

When high (> 10 km) antennas are involved, geometry based solely on the effective radius method may overestimate ray bending so that smooth earth horizon distances become excessive [31]. This difficulty is compensated for in IF-77 by the use of ray tracing in the determination of some key parameters such as effective terminal altitudes (Sec. 3.1), smooth earth horizon distances (Sec. 3.1), and effective distance (Sec. 10.1). In IF-77, ray tracing is performed through an exponential atmosphere [3, equations 3.43, 3.44, 3.40] in which the refractivity, N, varies with height above msl, h, as:

$$N = N_s \exp[-C_e (h - h_r)] \text{ N-units} \quad (17)$$

where

$$C_e = \log_e \left(\frac{N_s}{N_s + \Delta N} \right) \quad (18)$$

and

$$\Delta N = -7.32 \exp(0.005577\, N_s) \text{ N-units/km} \quad (19)$$

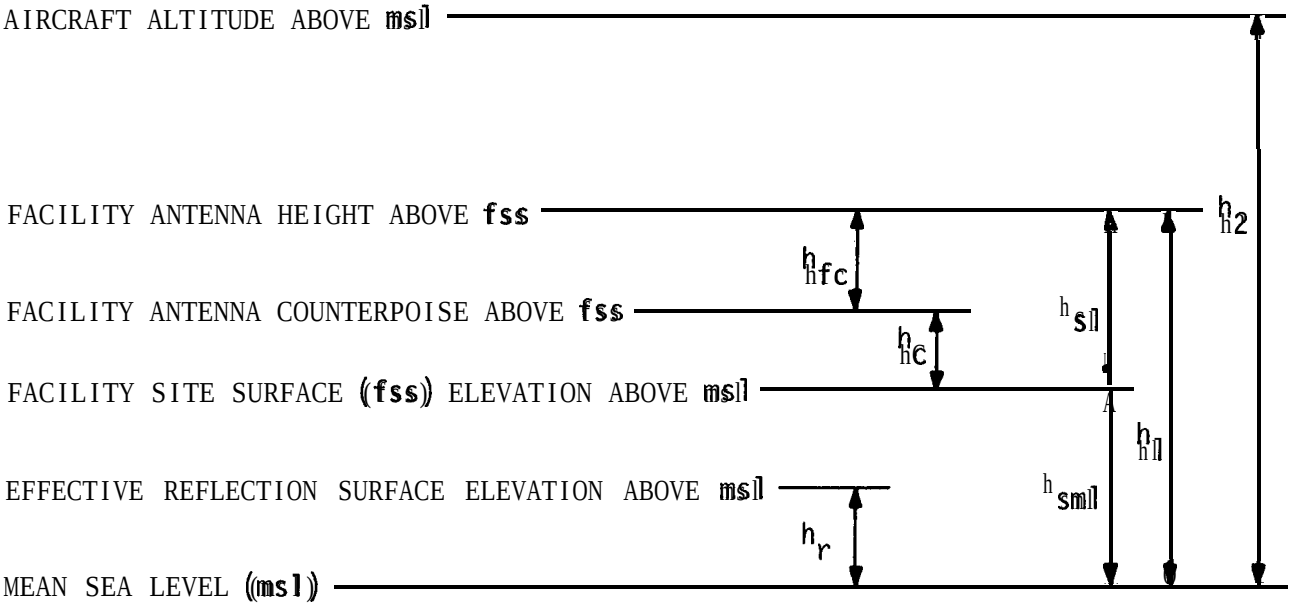

VALID INPUT CONSTRAINTS

$0 \leq h_r \leq 4$ km

$0 \leq h_{sml} \leq 4$ km

0.0005 km $< h_{sl}$

$h_{h1} \leq h_{h2}$

Note that aircraft altitude is elevation above msl while the facility antenna height is measured with respect to fss.

FIGURE 2. INPUT ANTENNA HEIGHTS AND SURFACE ELEVATIONS FOR IF-77.

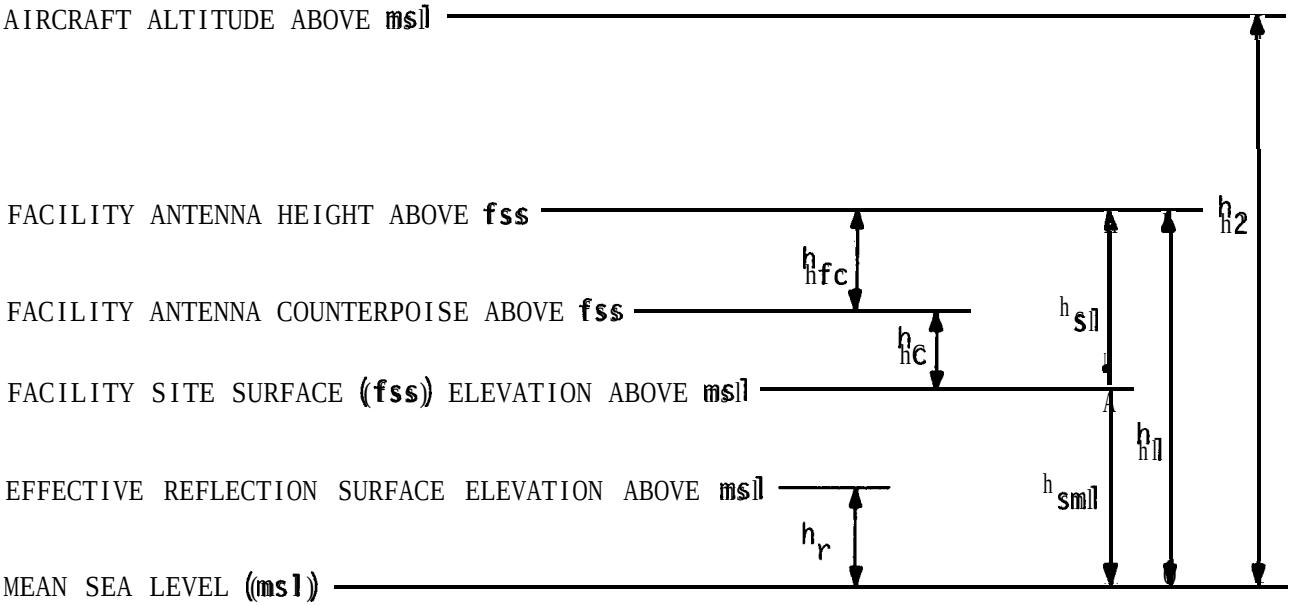

VALID INPUT CONSTRAINTS

$0 \leq h_r \leq 4$ km

$0 \leq h_{sml} \leq 4$ km

0.0005 km $< h_{sl}$

$h_{h1} \leq h_{h2}$

Note that aircraft altitude is elevation above msl while the facility antenna height is measured with respect to fss.

FIGURE 2. INPUT ANTENNA HEIGHTS AND SURFACE ELEVATIONS FOR IF-77.

$$\theta_{sR1,2} = d_{LsR1,2}/a \quad \text{rad} \tag{23}$$

$$h_{el,2} = \text{lesser of} \left[\begin{array}{l} h_{r1,2} \\ \text{or} \\ \left\{ \begin{array}{ll} 0.5\, d^2_{LsR1,2}/a & \text{if } \theta_{sR1,2} \geq 0.1 \text{ rad} \\ a[\sec(\theta_{sR1,2}) - 1] & \text{otherwise} \end{array} \right\} \end{array} \right] \quad \text{km} \tag{24}$$

$$\Delta h_{el,2} = h_{r1,2} - h_{el,2} \quad \text{km} \tag{25}$$

The final value of a smooth earth horizon distance, $d_{LS1,2}$, is taken as the ray tracing value for high antennas ($\Delta h_{el,2} > 0$) or computed via effective earth radius geometry, $d_{LsEl,2}$; i.e.:

$$d_{LsEl,2} = \sqrt{2a\, h_{el,2}} \quad \text{km} \tag{26}$$

$$d_{Ls1,2} = \left\{ \begin{array}{ll} d_{LsR1,2} & \text{if } \Delta h_{el,2} \geq 0 \\ d_{LsEl,2} & \text{otherwise} \end{array} \right\} \quad \text{km} \tag{27}$$

$$d_{Ls} = d_{Ls1} + d_{Ls2} \quad \text{km} \tag{28}$$

In addition, the ray elevation angle $\theta_{esR1,2}$ resulting from ray tracing is taken as the final ray elevation angle when $\Delta h_{el,2} > 0$; i.e.:

$$\theta_{s1,2} = d_{Ls1,2}/a \quad \text{rad} \tag{29}$$

$$\theta_{es1,2} = \left\{ \begin{array}{ll} \theta_{esR1,2} & \text{if } \Delta h_{el,2} > 0 \\ -\theta_{s1,2} & \text{otherwise} \end{array} \right\} \quad \text{rad} \tag{30}$$

$$\theta_{sR1,2} = d_{LsR1,2}/a \quad \text{rad} \tag{23}$$

$$h_{el,2} = \text{lesser of} \left[\begin{array}{l} h_{r1,2} \\ \text{or} \\ \left\{ \begin{array}{ll} 0.5\, d^2_{LsR1,2}/a & \text{if } \theta_{sR1,2} \geq 0.1 \text{ rad} \\ a[\sec(\theta_{sR1,2}) - 1] & \text{otherwise} \end{array} \right\} \end{array} \right] \quad \text{km} \tag{24}$$

$$\Delta h_{el,2} = h_{r1,2} - h_{el,2} \quad \text{km} \tag{25}$$

The final value of a smooth earth horizon distance, $d_{LS1,2}$, is taken as the ray tracing value for high antennas ($\Delta h_{el,2} > 0$) or computed via effective earth radius geometry, $d_{LsEl,2}$; i.e.:

$$d_{LsEl,2} = \sqrt{2a\, h_{el,2}} \quad \text{km} \tag{26}$$

$$d_{Ls1,2} = \left\{ \begin{array}{ll} d_{LsR1,2} & \text{if } \Delta h_{el,2} > 0 \\ d_{LsEl,2} & \text{otherwise} \end{array} \right\} \quad \text{km} \tag{27}$$

$$d_{Ls} = d_{Ls1} + d_{Ls2} \quad \text{km} \tag{28}$$

In addition, the ray elevation angle $\theta_{esR1,2}$ resulting from ray tracing is taken as the final ray elevation angle when $\Delta h_{el,2} > 0$; i.e.:

$$\theta_{s1,2} = d_{Ls1,2}/a \quad \text{rad} \tag{29}$$

$$\theta_{es1,2} = \left\{ \begin{array}{ll} \theta_{esR1,2} & \text{if } \Delta h_{el,2} > 0 \\ \theta_{s1,2} & \text{otherwise} \end{array} \right\} \quad \text{rad} \tag{30}$$

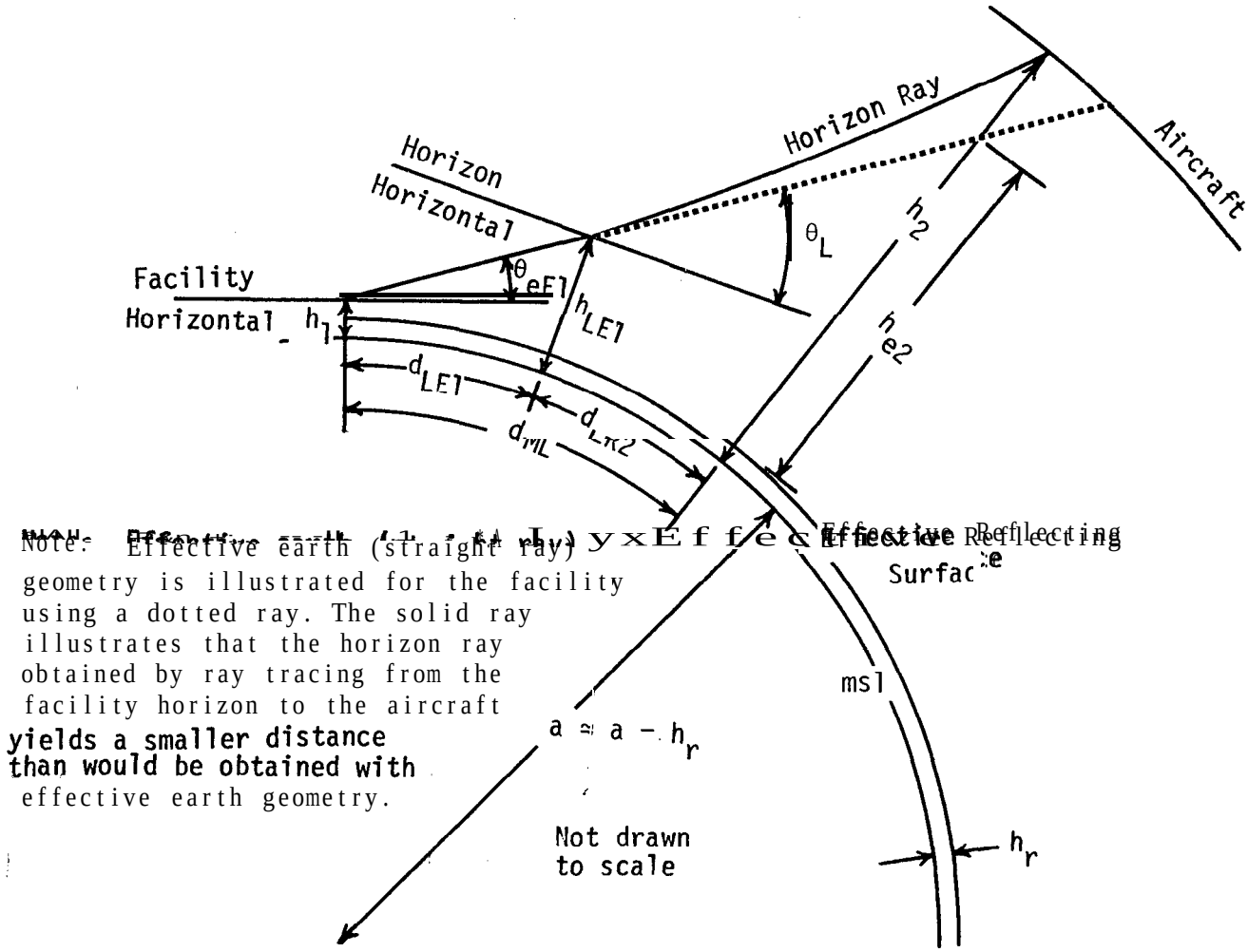

Note: Effective earth (straight ray) geometry is illustrated for the facility using a dotted ray. The solid ray illustrates that the horizon ray obtained by ray tracing from the facility horizon to the aircraft yields a smaller distance than would be obtained with effective earth geometry.

FIGURE 4. FACILITY RADIO HORIZON GEOMETRY.

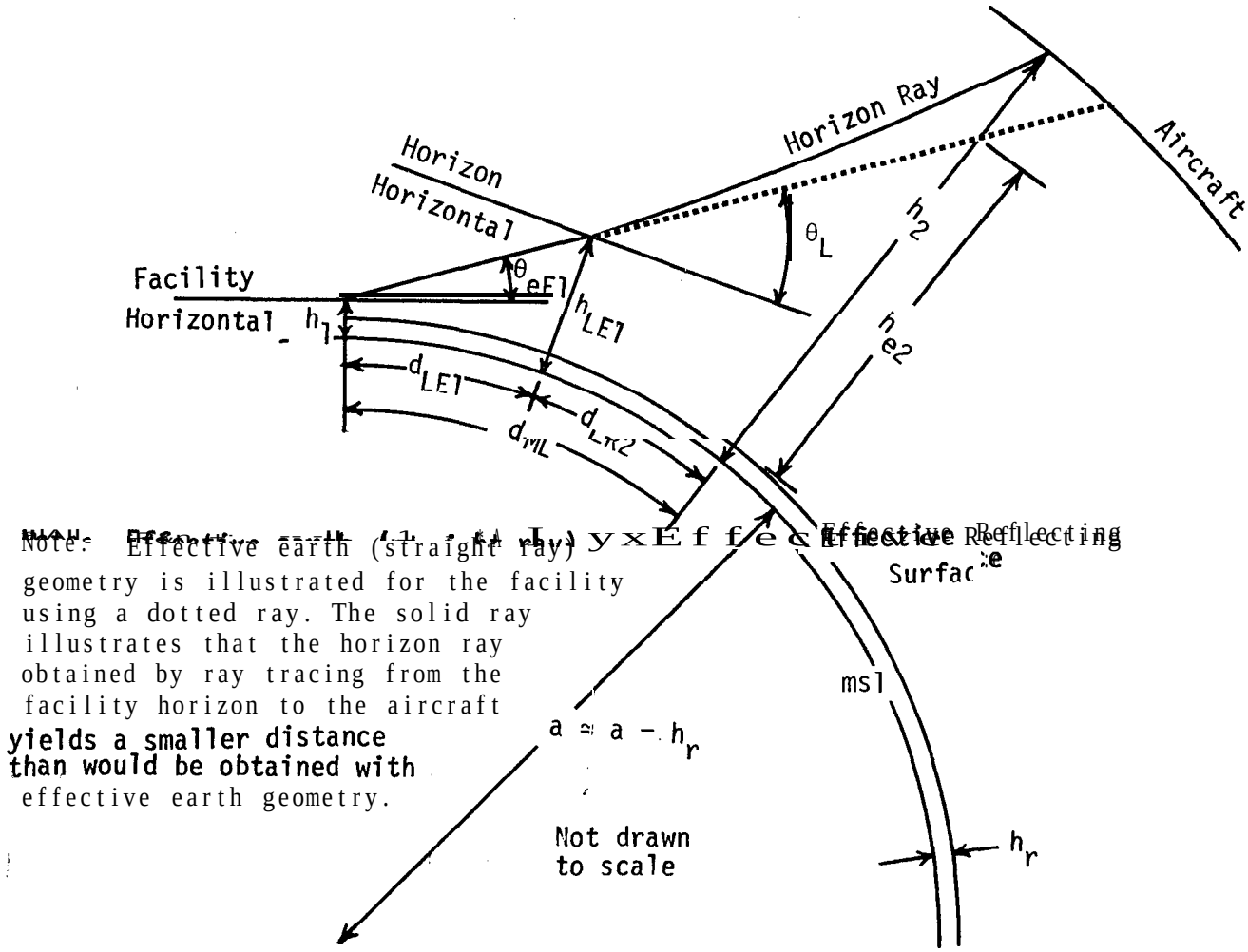

Note: Effective earth (straight ray) geometry is illustrated for the facility using a dotted ray. The solid ray illustrates that the horizon ray obtained by ray tracing from the facility horizon to the aircraft yields a smaller distance than would be obtained with effective earth geometry.

FIGURE 4. FACILITY RADIO HORIZON GEOMETRY.

$$\theta_{el} = \begin{cases} \theta_{eEl} \text{ if } \Delta h_{el} = 0 \\ \text{otherwise use ray tracing} \end{cases} \quad (40)$$

$$d_{Ll} = \begin{cases} d_{LEl} \text{ iff } \Delta h_{el} = 0 \\ \text{otherwise use ray tracing} \end{cases} \quad (41)$$

The ray tracing referred to in (40) and (41) is started at the horizon elevation, h_{Lrl}, with a take-off angle of $-\theta_L$ and continues until the facility antenna height h_{rl} is reached. Then, the great-circle distance traversed by the ray is taken as d_{Ll}; and the negative of the ray arrival angle is taken as θ_{el}. The take-off angle used is calculated from:

$$\theta_L = \theta_{eEl} + \left(d_{LEl}/a\right) \quad (42)$$

Figure 5 provides a summary of the logic used for facility horizon determination.

The distance d_{LR2} shown in Figure 4 is taken as the distance under a ray traced from the facility horizon with a take-off angle of θ_L from (42) to the aircraft altitude of h_2. This distance is then used with $d_{Ls1,2}$ from (27) to calculate the maximum line-of-sight distance d_{ML} which is also shown in Figure 4; i.e.:

$$d_{ML} = \left\{ \begin{array}{l} d_{Ls1} + d_{Ls2} \text{ for smooth earth; i.e., } \Delta h = 0 \\ a\left(\cos^{-1}\left(\dfrac{(a + h_{el})\cos\theta_{el}}{(a + h_{e2})}\right) - \theta_{el}\right) \text{ if } \Delta h_{e2} = 0 \\ d_{L1} + d_{LR2} \quad \text{otherwise} \end{array} \right\} \text{ km} \quad (43)$$

3.3 Aircraft (Or Higher Antenna) Horizon

Aircraft horizon parameters are determined using either (a) case 1, where the facility horizon obstacle is assumed to provide the aircraft radio horizon, or (b) case 2, where the effective reflection surface is assumed to provide the aircraft

$$\theta_{el} = \begin{cases} \theta_{eEl} \text{ if } \Delta h_{el} = 0 \\ \text{otherwise use ray tracing} \end{cases} \quad (40)$$

$$d_{Ll} = \begin{cases} d_{LEl} \text{ iff } \Delta h_{el} = 0 \\ \text{otherwise use ray tracing} \end{cases} \quad (41)$$

The ray tracing referred to in (40) and (41) is started at the horizon elevation, h_{Lrl}, with a take-off angle of $-\theta_L$ and continues until the facility antenna height h_{rl} is reached. Then, the great-circle distance traversed by the ray is taken as d_{Ll}; and the negative of the ray arrival angle is taken as θ_{el}. The take-off angle used is calculated from:

$$\theta_L = \theta_{eEl} + \left(d_{LEl}/a\right) \quad (42)$$

Figure 5 provides a summary of the logic used for facility horizon determination.

The distance d_{LR2} shown in Figure 4 is taken as the distance under a ray traced from the facility horizon with a take-off angle of θ_L from (42) to the aircraft altitude of h_2. This distance is then used with $d_{Ls1,2}$ from (27) to calculate the maximum line-of-sight distance d_{ML} which is also shown in Figure 4; i.e.:

$$d_{ML} = \left\{ \begin{array}{l} d_{Ls1} + d_{Ls2} \text{ for smooth earth; i.e., } \Delta h = 0 \\ a\left(\cos^{-1}\left(\dfrac{(a + h_{el})\cos\theta_{el}}{(a + h_{e2})}\right) - \theta_{el}\right) \text{ if } \Delta h_{e2} = 0 \\ d_{L1} + d_{LR2} \quad \text{otherwise} \end{array} \right\} \text{ km} \quad (43)$$

3.3 Aircraft (Or Higher Antenna) Horizon

Aircraft horizon parameters are determined using either (a) case 1, where the facility horizon obstacle is assumed to provide the aircraft radio horizon, or (b) case 2, where the effective reflection surface is assumed to provide the aircraft

with a smooth-earth radio horizon. The great-circle horizon distance for the aircraft, d_{L2}, is calculated using the parameters shown in Figure 6 along with the great-circle distance, d, between the facility and the aircraft; i.e.:

$$d_{sL} = \sqrt{2a\, h_{Lr1}} \quad km \tag{44}$$

$$d_{LM} = d_{L1} + d_{sL} + d_{Ls2} \quad km \tag{45}$$

$$d_{L2} = \begin{cases} d - d_{L1} & \text{if } d_{ML} \leq d \leq d_{LM} \\ d_{Ls2} & \text{otherwise} \end{cases} \quad km \tag{46}$$

Here, h_{Lr1} is the height of the facility horizon obstacle above the effective reflection surface from Figure 5, and d_{sL} is the smooth-earth horizon distance for the obstacle (i.e., a is from (16), d_{L1} is from (41), and d_{Ls2} is from (27)). The horizon ray elevation angle at the aircraft, θ_{e2}, is measured relative to the horizontal at the aircraft, with positive values assigned to values above the horizontal. It is calculated from:

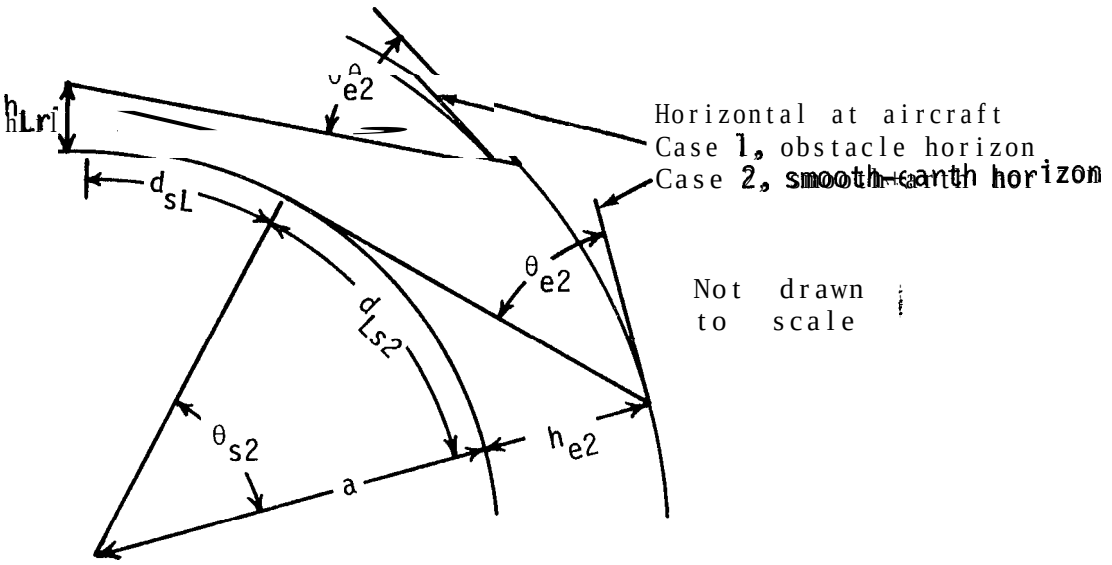

FIGURE 6. GEOMETRY FOR AIRCRAFT RADIO HORIZON

with a smooth-earth radio horizon. The great-circle horizon distance for the aircraft, d_{L2}, is calculated using the parameters shown in Figure 6 along with the great-circle distance, d, between the facility and the aircraft; i.e.:

$$d_{sL} = \sqrt{2a\, h_{Lr1}} \quad km \tag{44}$$

$$d_{LM} = d_{L1} + d_{sL} + d_{Ls2} \quad km \tag{45}$$

$$d_{L2} = \begin{cases} d - d_{L1} & \text{if } d_{ML} \leq d \leq d_{LM} \\ d_{Ls2} & \text{otherwise} \end{cases} \quad km \tag{46}$$

Here, h_{Lr1} is the height of the facility horizon obstacle above the effective reflection surface from Figure 5, and d_{sL} is the smooth-earth horizon distance for the obstacle (i.e., a is from (16), d_{L1} is from (41), and d_{Ls2} is from (27)). The horizon ray elevation angle at the aircraft, θ_{e2}, is measured relative to the horizontal at the aircraft, with positive values assigned to values above the horizontal. It is calculated from:

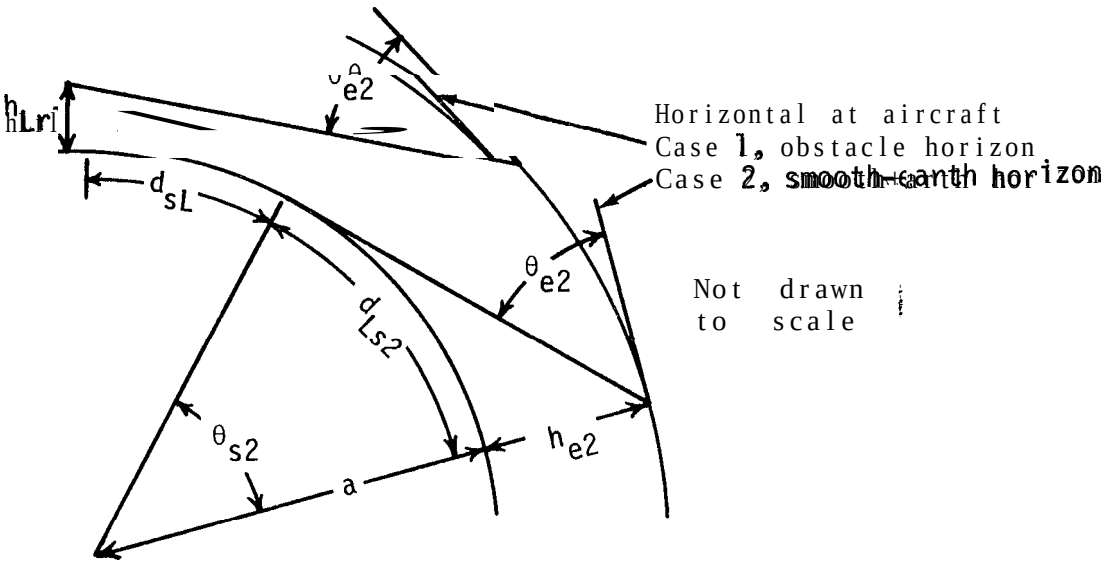

FIGURE 6. GEOMETRY FOR AIRCRAFT RADIO HORIZON

F-O-A for d_A where d_{ML} corresponds to the maximum line-of-sight distance and d_A is the shortest beyond-the-horizon distance that involves both the facility horizon obstacle and a smooth-earth horizon for the aircraft.

Rounded-earth and knife-edge diffraction calculations are discussed in Sections 4.1 and 4.2, respectively. Section 4.3 deals with the determination of the diffraction attenuation, A_d.

4.1 Rounded-Earth Diffraction

Rounded-earth diffraction calculations in IF-77 involve the determination of straight-line attenuation versus distance parameters for paths F-O-ML and O-A of Figure 7. Key parameters for these calculations are as follows:

$$h_{ep1} \equiv \left\{ \begin{array}{l} h_{e1} \text{ from (24) for path F-O-ML} \\ h_{Lr1} \text{ from (39) for path O-A} \end{array} \right\} \text{ km} \qquad (50)$$

$$h_{ep2} \equiv h_{e2} \text{ km from (24) for both paths} \qquad (51)$$

$$d_{Lp1} = \left\{ \begin{array}{l} d_{L1} \text{ from (41) for path F-O-ML} \\ d_{Lo1} = d_{sL} \text{ from (44) for path O-A} \end{array} \right\} \text{ km} \qquad (52)$$

$$d_{Lp2} = \left\{ \begin{array}{l} d_{ML} - d_{L1} \text{ for path F-O-ML} \\ \quad \text{with } d_{ML} \text{ from (43)} \\ d_{Lo2} = d_{Ls2} \text{ from (27) for path O-A} \end{array} \right\} \text{ km} \qquad (53)$$

$$A_p = \left\{ \begin{array}{l} \text{Attenuation line intercept} \\ A_f \text{ for path F-O-ML} \\ A_o \text{ for path O-A} \end{array} \right\} \text{ dB} \qquad (54)$$

F-O-A for d_A where d_{ML} corresponds to the maximum line-of-sight distance and d_A is the shortest beyond-the-horizon distance that involves both the facility horizon obstacle and a smooth-earth horizon for the aircraft.

Rounded-earth and knife-edge diffraction calculations are discussed in Sections 4.1 and 4.2, respectively. Section 4.3 deals with the determination of the diffraction attenuation, A_d.

4.1 Rounded-Earth Diffraction

Rounded-earth diffraction calculations in IF-77 involve the determination of straight-line attenuation versus distance parameters for paths F-O-ML and O-A of Figure 7. Key parameters for these calculations are as follows:

$$h_{ep1} \equiv \left\{ \begin{array}{l} h_{e1} \text{ from (24) for path F-O-ML} \\ h_{Lr1} \text{ from (39) for path O-A} \end{array} \right\} \text{ km} \qquad (50)$$

$$h_{ep2} \equiv h_{e2} \text{ km from (24) for both paths} \qquad (51)$$

$$d_{Lp1} = \left\{ \begin{array}{l} d_{L1} \text{ from (41) for path F-O-ML} \\ d_{Lo1} = d_{sL} \text{ from (44) for path O-A} \end{array} \right\} \text{ km} \qquad (52)$$

$$d_{Lp2} = \left\{ \begin{array}{l} d_{ML} - d_{L1} \text{ for path F-O-ML} \\ \quad \text{with } d_{ML} \text{ from (43)} \\ d_{Lo2} = d_{Ls2} \text{ from (27) for path O-A} \end{array} \right\} \text{ km} \qquad (53)$$

$$A_p = \left\{ \begin{array}{l} \text{Attenuation line intercept} \\ A_f \text{ for path F-O-ML} \\ A_o \text{ for path O-A} \end{array} \right\} \text{ dB} \qquad (54)$$

$$K_{d1,2,3,4} = 0.36278\,(fa_{1,2,3,4})^{-1/3}\left[(\epsilon - 1)^2 + x^2\right]^{-1/4} \tag{65}$$

$$K_{1,2,3,4} = \begin{cases} K_{d1,2,3,4} & \text{for horizontal polarization} \\ \text{or} & \\ K_{d1,2,3,4}\left[b^2 + x^2\right]^{1/2} & \text{for vertical polarization} \end{cases} \tag{66}$$

$$K_{F1,2} = \text{smaller of } (K_{1,2} \text{ or } 0.99999) \tag{67}$$

$$B_{1,2,3,4} = 416.4 f^{1/3}(1.607 - K_{1,2,3,4}) \tag{68}$$

$$X_{1,2} = B_{1,2} a_{1,2}^{-2/3} d_{Lp1,2} \quad \text{km} \tag{69}$$

$$X_{3,4} = B_{3,4} a_{3,4}^{-2/3} (d_{3,4} - d_{Lp}) + X_1 + X_2 \quad \text{km} \tag{70}$$

$$G_{1,2,3,4} = 0.0575 X_{1,2,3,4} - 10 \log X_{1,2,3,4} \tag{71}$$

$$W_{1,2} = 0.0134 X_{1,2} \exp(-0.005 X_{1,2}) \tag{72}$$

$$y_{1,2} = 40 \log (X_{1,2}) - 117 \quad \text{dB} \tag{73}$$

$$F_{1,2} = \begin{cases} y_{1,2} \text{ or } -117 \text{ whichever has the smaller absolute value for } 0 \le K_{F1,2} \le 10^{-5} \\ \text{or} \\ y_{1,2} \text{ for } 10^{-5} \le K_{F1,2} \text{ and} \\ \qquad -450\left(\log K_{F1,2}\right)^{-3} \le X_{1,2} \\ \text{or} \\ 20 \log (K_{F1,2}) - 15 + 2.5\,(10^{-5}) X_{1,2}^2 / K_{F1,2} \\ \qquad \text{otherwise} \end{cases} \quad \text{dB} \tag{74}$$

$$K_{d1,2,3,4} = 0.36278\,(fa_{1,2,3,4})^{-1/3}\left[(\epsilon - 1)^2 + x^2\right]^{-1/4} \tag{65}$$

$$K_{1,2,3,4} = \begin{cases} K_{d1,2,3,4} & \text{for horizontal polarization} \\ \text{or} & \\ K_{d1,2,3,4}\left[b^2 + x^2\right]^{1/2} & \text{for vertical polarization} \end{cases} \tag{66}$$

$$K_{F1,2} = \text{smaller of } (K_{1,2} \text{ or } 0.99999) \tag{67}$$

$$B_{1,2,3,4} = 416.4 f^{1/3}(1.607 - K_{1,2,3,4}) \tag{68}$$

$$X_{1,2} = B_{1,2} a_{1,2}^{-2/3} d_{Lp1,2} \quad \text{km} \tag{69}$$

$$X_{3,4} = B_{3,4} a_{3,4}^{-2/3} (d_{3,4} - d_{Lp}) + X_1 + X_2 \quad \text{km} \tag{70}$$

$$G_{1,2,3,4} = 0.0575 X_{1,2,3,4} - 10 \log X_{1,2,3,4} \tag{71}$$

$$W_{1,2} = 0.0134 X_{1,2} \exp(-0.005 X_{1,2}) \tag{72}$$

$$y_{1,2} = 40 \log (X_{1,2}) - 117 \quad \text{dB} \tag{73}$$

$$F_{1,2} = \begin{cases} y_{1,2} \text{ or } -117 \text{ whichever has the smaller absolute value for } 0 \le K_{F1,2} \le 10^{-5} \\ \text{or} \\ y_{1,2} \text{ for } 10^{-5} \le K_{F1,2} \text{ and} \\ \qquad -450\left(\log K_{F1,2}\right)^{-3} \le X_{1,2} \\ \text{or} \\ 20 \log (K_{F1,2}) - 15 + 2.5\,(10^{-5}) X_{1,2}^2 / K_{F1,2} \\ \qquad \text{otherwise} \end{cases} \quad \text{dB} \tag{74}$$

Whenever $h_{epl,2} \geq 2 f_{ch,2}$

0

or when $\bar{h}_{1,2} \geq 2.5$

$-6.6 - 0.013 \bar{h}_{1,2} - 2 \log \bar{h}_{1,2}$

or when $K_{1,2} \geq 0.01$

$1.2 - 13.5 \bar{h}_{1,2} + 15 \log \bar{h}_{1,2}$ if $\bar{h}_{1,2} < 0.3$

$-6.5 - 1.67 \bar{h}_{1,2} + 6.8 \log \bar{h}_{1,2}$ if $\bar{h}_{1,2} \geq 0.3$

or when $0.01 < K_{1,2} \leq 0.05$

$T - 25 (T - B) (0.05 - K_{1,2})$

$G_{\bar{h}1,2} =$ where dB (83)

$T = -13.9 + 24.1 \bar{h}_{1,2} + 3.1 \log \bar{h}_{1,2}$ if $\bar{h}_{1,2} < 0.25$

$T = -5.9 - 1.9 \bar{h}_{1,2} + 6.6 \log \bar{h}_{1,2}$ if $\bar{h}_{1,2} \geq 0.25$

$B = 1.2 - 13.5 \bar{h}_{1,2} + 15 \log \bar{h}_{1,2}$ if $\bar{h}_{1,2} < 0.3$

$B = -6.5 - 1.67 \bar{h}_{1,2} + 6.8 \log \bar{h}_{1,2}$ if $\bar{h}_{1,2} \geq 0.3$

or when $K_{1,2} > 0.05$

$T - 20 (T - B) (0.1 - K_{1,2})$

where

$T = -13$ if $\bar{h}_{1,2} < 0.1$

$T = -4.7 - 2.5 \bar{h}_{1,2} + 7.6 \log \bar{h}_{1,2}$ if $\bar{h}_{1,2} \geq 0.1$

$B = -13.9 + 24.1 \bar{h}_{1,2} + 3.1 \log \bar{h}_{1,2}$ if $\bar{h}_{1,2} < 0.25$

$B = -5.9 - 1.9 \bar{h}_{1,2} + 6.6 \log \bar{h}_{1,2}$ if $\bar{h}_{1,2} \geq 0.25$

$G_{\bar{h}pl,2} = \left(G_{hl,2}\right)\left(G_{Wl,2}\right)$ dB (84)

Whenever $h_{epl,2} \geq 2 f_{ch,2}$

$$G_{hpl,2} = 0$$

or when $\bar{h}_{1,2} \geq 2.5$

$$G_{hpl,2} = -6.6 - 0.013 \bar{h}_{1,2} - 2 \log \bar{h}_{1,2}$$

or when $K_{1,2} \geq 0.01$

$$G_{hpl,2} = 1.2 - 13.5 \bar{h}_{1,2} + 15 \log \bar{h}_{1,2} \quad \text{if } \bar{h}_{1,2} < 0.3$$

$$G_{hpl,2} = -6.5 - 1.67 \bar{h}_{1,2} + 6.8 \log \bar{h}_{1,2} \quad \text{if } \bar{h}_{1,2} \geq 0.3$$

or when $0.01 < K_{1,2} \leq 0.05$

$$G_{hpl,2} = T - 25 (T - B) (0.05 - K_{1,2})$$

where

$$T = -13.9 + 24.1 \bar{h}_{1,2} + 3.1 \log \bar{h}_{1,2} \quad \text{if } \bar{h}_{1,2} < 0.25$$

$$T = -5.9 - 1.9 \bar{h}_{1,2} + 6.6 \log \bar{h}_{1,2} \quad \text{if } \bar{h}_{1,2} \geq 0.25$$

$$B = 1.2 - 13.5 \bar{h}_{1,2} + 15 \log \bar{h}_{1,2} \quad \text{if } \bar{h}_{1,2} < 0.3$$

$$B = -6.5 - 1.67 \bar{h}_{1,2} + 6.8 \log \bar{h}_{1,2} \quad \text{if } \bar{h}_{1,2} \geq 0.3$$

or when $K_{1,2} > 0.05$

$$G_{hpl,2} = T - 20 (T - B) (0.1 - K_{1,2})$$

where

$$T = -13 \quad \text{if } \bar{h}_{1,2} < 0.1$$

$$T = -4.7 - 2.5 \bar{h}_{1,2} + 7.6 \log \bar{h}_{1,2} \quad \text{if } \bar{h}_{1,2} \geq 0.1$$

$$B = -13.9 + 24.1 \bar{h}_{1,2} + 3.1 \log \bar{h}_{1,2} \quad \text{if } \bar{h}_{1,2} < 0.25$$

$$B = -5.9 - 1.9 \bar{h}_{1,2} + 6.6 \log \bar{h}_{1,2} \quad \text{if } \bar{h}_{1,2} \geq 0.25$$

$$G_{hpl,2} = \left(G_{hl,2}\right)\left(G_{Wl,2}\right) \quad \text{dB} \tag{84}$$

$$\theta_v = \theta_{e1} + \theta_{es2} + \theta_{L1} + \theta_{LsA} \quad \text{rad} \tag{89}$$

$$v = 5.1658 \sin(0.5\theta_v)\sqrt{f d_{L1} d_{LsA}/(d_{L1} + d_{LsA})} \tag{90}$$

$$C_v = \int_0^v \cos\left(\frac{\pi t^2}{2}\right) dt, \quad S_v = \int_0^v \sin\left(\frac{\pi t^2}{2}\right) dt \tag{91}$$

where these are Fresnel integrals [34, p. III-18].

$$f_{rv} = 0.5 \sqrt{[1 - (C_v + S_v)]^2 + (C_v - S_v)^2} \tag{92}$$

$$A_{KA} = A_{r0} - G_{rf1} - G_{r01} - 20 \log f_v \quad \text{dB} \tag{93}$$

4.3 Diffraction Attenuation, A_d

Diffraction attenuation, A_d, is calculated using the rounded-earth diffraction (Sec. 4.1) and knife-edge diffraction (Sec. 4.2) parameters just discussed; i.e.

$$W = \left\{ \begin{array}{l} 1 \text{ when } d_{ML} \geq d_{Ls} \text{ (rounded-earth only)} \\ 0 \text{ when } d_{ML} \leq 0.9\, d_{Ls} \text{ (knife-edge only)} \\ 0.5\left(1 + \cos\left(\dfrac{\pi(d_{Ls} - d_{ML})}{0.1\, d_{Ls}}\right)\right) \quad \text{otherwise} \\ \text{(combination of both)} \end{array} \right\} \tag{94}$$

where the maximum line-of-sight distance, d_{ML}, is from (43), and the total smooth-earth horizon distance, d_{Ls}, is from (28):

$$A_{ML} = \left\{ \begin{array}{l} \text{if } A_{rML} \text{ if } W > 0.999 \\ A_{KML} \text{ if } W < 0.001 \quad \text{dB} \\ (1 - W)\, A_{KML} + W A_{rML} \text{ otherwise} \end{array} \right\} \tag{95}$$

where $A_{rML} \equiv A_{rE}$ from (85) with $d = d_{ML}$ and A_{KML} is from (87).

$$d_A = d_{L1} + d_{LsA} \quad \text{km} \tag{96}$$

$$\theta_v = \theta_{e1} + \theta_{es2} + \theta_{L1} + \theta_{LsA} \quad \text{rad} \tag{89}$$

$$v = 5.1658 \sin(0.5\theta_v)\sqrt{f d_{L1} d_{LsA}/(d_{L1} + d_{LsA})} \tag{90}$$

$$C_v = \int_0^v \cos\left(\frac{\pi t^2}{2}\right) dt, \quad S_v = \int_0^v \sin\left(\frac{\pi t^2}{2}\right) dt \tag{91}$$

where these are Fresnel integrals [34, p. III-18].

$$f_{rv} = 0.5 \sqrt{[1 - (C_v + S_v)]^2 + (C_v - S_v)^2} \tag{92}$$

$$A_{KA} = A_{r0} - G_{rf1} - G_{r01} - 20 \log f_v \quad \text{dB} \tag{93}$$

4.3 Diffraction Attenuation, A_d

Diffraction attenuation, A_d, is calculated using the rounded-earth diffraction (Sec. 4.1) and knife-edge diffraction (Sec. 4.2) parameters just discussed; i.e.

$$W = \left\{ \begin{array}{l} 1 \text{ when } d_{ML} \geq d_{Ls} \text{ (rounded-earth only)} \\ 0 \text{ when } d_{ML} \leq 0.9\, d_{Ls} \text{ (knife-edge only)} \\ 0.5\left(1 + \cos\left(\dfrac{\pi(d_{Ls} - d_{ML})}{0.1\, d_{Ls}}\right)\right) \quad \text{otherwise} \\ \text{(combination of both)} \end{array} \right\} \tag{94}$$

where the maximum line-of-sight distance, d_{ML}, is from (43), and the total smooth-earth horizon distance, d_{Ls}, is from (28):

$$A_{ML} = \left\{ \begin{array}{l} \text{if } A_{rML} \text{ if } W > 0.999 \\ A_{KML} \text{ if } W < 0.001 \quad \text{dB} \\ (1 - W)\, A_{KML} + W A_{rML} \text{ otherwise} \end{array} \right\} \tag{95}$$

where $A_{rML} \equiv A_{rE}$ from (85) with $d = d_{ML}$ and A_{KML} is from (87).

$$d_A = d_{L1} + d_{LsA} \quad \text{km} \tag{96}$$

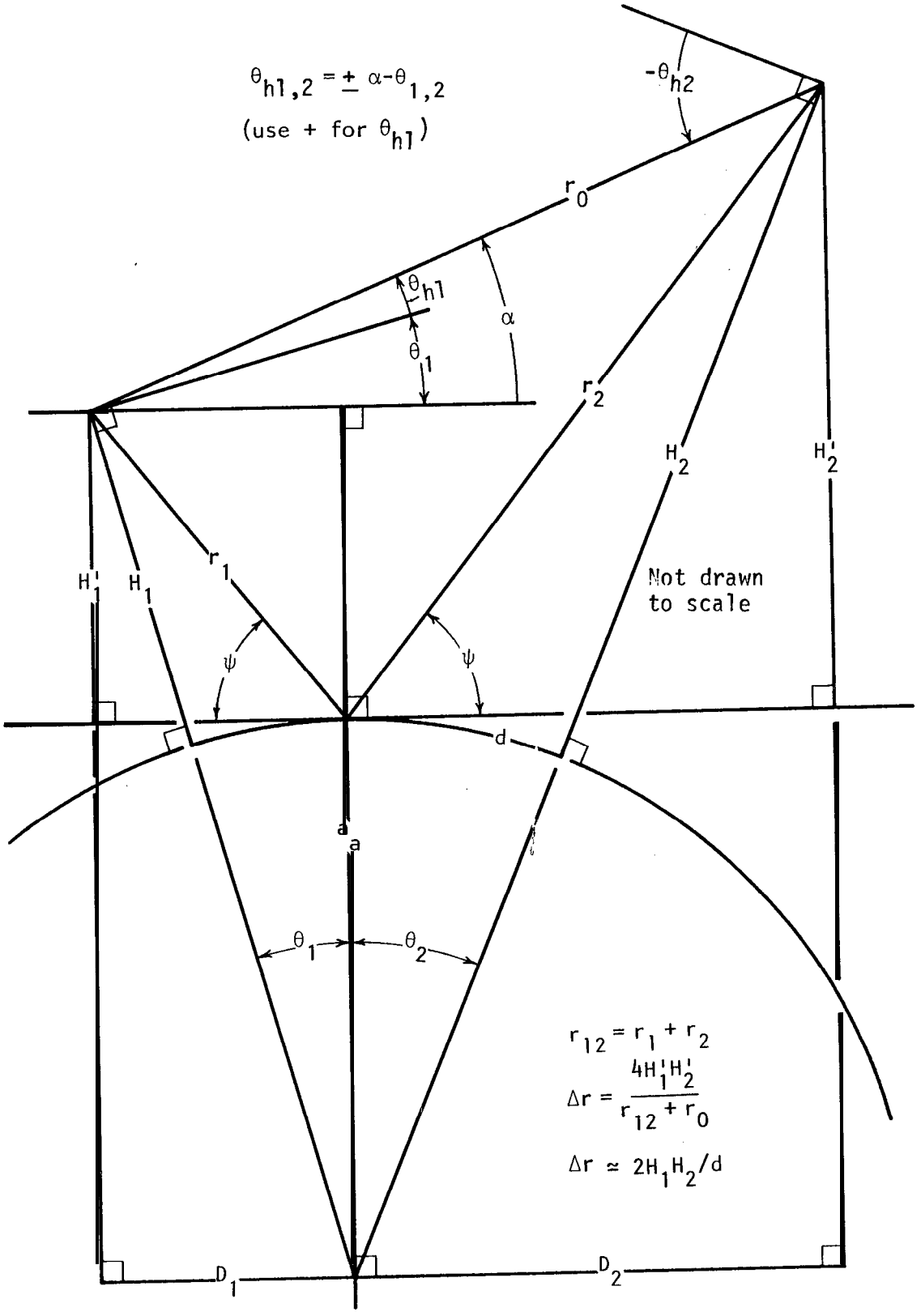

Note: Relationships between the various geometric parameters shown here were previously provided in IF-73 [14], Sec. A.4.2.

FIGURE 8. SPHERICAL EARTH GEOMETRY.

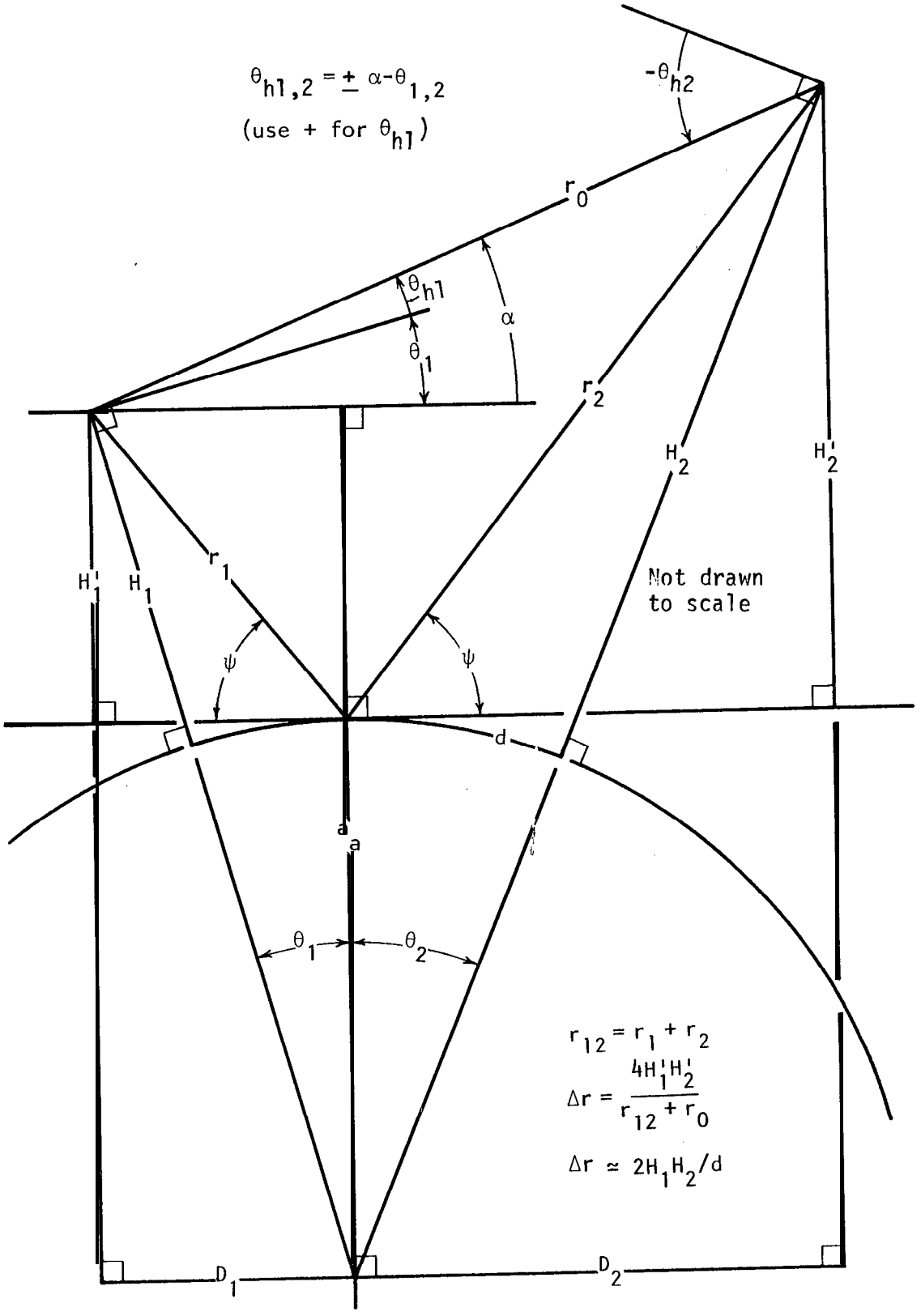

Note: Relationships between the various geometric parameters shown here were previously provided in IF-73 [14], Sec. A.4.2.

FIGURE 8. SPHERICAL EARTH GEOMETRY.

$$H'_{i,2} = \begin{cases} D_{1,2} \tan \psi \text{ for } \psi < 1.56 \text{ rad} \\ H_{1,2} \quad \text{otherwise} \end{cases} \quad \text{km} \tag{110}$$

$$\alpha = \begin{cases} \text{Tan}^{-1}[(H'_2 - H'_1)/(D_1 + D_2)] \text{ for } \psi < 1.56 \text{ rad} \\ \psi \quad \text{otherwise} \end{cases} \quad \text{km} \tag{111}$$

$$r_0 = \begin{cases} (D_1 + D_2)/\cos \alpha \text{ for } \psi < 1.56 \text{ rad} \\ H_2 - H_1 \quad \text{otherwise} \end{cases} \quad \text{km} \tag{112}$$

$$r_{12} = \begin{cases} (D_1 + D_2)/\cos \psi \text{ for } \psi < 1.56 \text{ rad} \\ H_1 + H_2 \quad \text{otherwise} \end{cases} \quad \text{km} \tag{113}$$

$$\Delta r = 4 H'_1 H'_2/(r_0 + r_{12}) \quad \text{km} \tag{114a}$$

Δr_g = Δr with earth parameters in (106) km (114b)

Δr_c = Δr with counterpoise parameters in (106) km (114c)

$$\theta_{h1} = \alpha - \theta_1 \quad \text{rad} \tag{115a}$$

$$\theta_{h2} = -(\alpha + \theta_2) \quad \text{rad} \tag{115b}$$

$$\theta_{r1,2} = -(\psi + \theta_{1,2}) \quad \text{rad} \tag{116}$$

$$\theta_0 = \theta_1 + \theta_2 \quad \text{rad} \tag{117}$$

$$d_1 = a_e \theta_0 \quad \text{km} \tag{118}$$

$$H'_{1,2} = \begin{cases} D_{1,2} \tan \psi & \text{for } \psi < 1.56 \text{ rad} \\ H_{1,2} & \text{otherwise} \end{cases} \quad \text{km} \tag{110}$$

$$\alpha = \begin{cases} \text{Tan}^{-1}[(H'_2 - H'_1)/(D_1 + D_2)] & \text{for } \psi < 1.56 \text{ rad} \\ \psi & \text{otherwise} \end{cases} \quad \text{km} \tag{111}$$

$$r_0 = \begin{cases} (D_1 + D_2)/\cos \alpha & \text{for } \psi < 1.56 \text{ rad} \\ H_2 - H_1 & \text{otherwise} \end{cases} \quad \text{km} \tag{112}$$

$$r_{12} = \begin{cases} (D_1 + D_2)/\cos \psi & \text{for } \psi < 1.56 \text{ rad} \\ H_1 + H_2 & \text{otherwise} \end{cases} \quad \text{km} \tag{113}$$

$$\Delta r = 4 H'_1 H'_2/(r_0 + r_{12}) \quad \text{km} \tag{114a}$$

$$\Delta r_g = \Delta r \text{ with earth parameters in (106)} \quad \text{km} \tag{114b}$$

$$\Delta r_c = \Delta r \text{ with counterpoise parameters in (106)} \quad \text{km} \tag{114c}$$

$$\theta_{h1} = \alpha - \theta_1 \quad \text{rad} \tag{115a}$$

$$\theta_{h2} = -(\alpha + \theta_2) \quad \text{rad} \tag{115b}$$

$$\theta_{r1,2} = -(\psi + \theta_{1,2}) \quad \text{rad} \tag{116}$$

$$\theta_0 = \theta_1 + \theta_2 \quad \text{rad} \tag{117}$$

$$d_1 = a \theta_0 \quad \text{km} \tag{118}$$

When both antennas are high and close (i.e., two close aircraft), the relative magnitude of the reflected ray will be reduced because the reflected ray length is much longer than the direct ray length (i.e., larger free space loss for reflected ray) [15, Sec. 3.3]. The ray length factor, F_r, in (119a) is used to account for this.

The formulation for D_v and F_r may be summarized as follows:

$$r_{1,2} = \left\{ \begin{array}{l} H_{1,2} \text{ if } \psi \simeq 90° \\ D_{1,2}/\cos\psi \text{ otherwise} \end{array} \right\} \text{ km} \qquad (120)$$

where $H_{1,2}$ are from (106); the grazing angle, ψ (Fig. 8), is a starting parameter for the Δr formulation of Section 5.1; and $D_{1,2}$ are from (109)

$$R_r = \frac{r_1 r_2}{r_{12}} \quad \text{km} \qquad (121)$$

where $r_{1,2}$ are from (120) and r_{12} is from (113)

$$D_v = \left[1 + \frac{2R_r(1 + \sin^2\psi)}{a_a \sin\psi} + \left(\frac{2R_r}{a_a} \right)^2 \right]^{-1/2} \qquad (122)$$

where a_a is from (104), and

$$F_r = r_0/r_{12} \qquad (123)$$

where r_0 is from (112).

5.2.2 Surface Roughness Factors

Surface roughness factors for specular, F_{soh}, and diffuse, F_{doh}, reflections are calculated as follows:

$$\Delta h_d = \Delta h_m [1 - 0.8 \exp(-0.02d)] \text{ m} \qquad (124)$$

When both antennas are high and close (i.e., two close aircraft), the relative magnitude of the reflected ray will be reduced because the reflected ray length is much longer than the direct ray length (i.e., larger free space loss for reflected ray) [15, Sec. 3.3]. The ray length factor, F_r, in (119a) is used to account for this.

The formulation for D_v and F_r may be summarized as follows:

$$r_{1,2} = \left\{ \begin{array}{l} H_{1,2} \text{ if } \psi \simeq 90° \\ D_{1,2}/\cos\psi \text{ otherwise} \end{array} \right\} \text{ km} \qquad (120)$$

where $H_{1,2}$ are from (106); the grazing angle, ψ (Fig. 8), is a starting parameter for the Δr formulation of Section 5.1; and $D_{1,2}$ are from (109)

$$R_r = \frac{r_1 r_2}{r_{12}} \quad \text{km} \qquad (121)$$

where $r_{1,2}$ are from (120) and r_{12} is from (113)

$$D_v = \left[1 + \frac{2R_r(1 + \sin^2\psi)}{a_a \sin\psi} + \left(\frac{2R_r}{a_a} \right)^2 \right]^{-1/2} \qquad (122)$$

where a_a is from (104), and

$$F_r = r_0/r_{12} \qquad (123)$$

where r_0 is from (112).

5.2.2 Surface Roughness Factors

Surface roughness factors for specular, F_{soh}, and diffuse, F_{doh}, reflections are calculated as follows:

$$\Delta h_d = \Delta h_m [1 - 0.8 \exp(-0.02d)] \text{ m} \qquad (124)$$

5.2.3 Counterpoise Factors

Counterpoise factor, f_g, in (119a) is used to provide some reduction in the reflection from the earth's surface when this reflecting surface is shadowed by the counterpoise. Counterpoise factor, f_c, in (119b) is used to provide some reduction in the reflection from the counterpoise because of the limited area of the counterpoise. When there is no counterpoise, $f_g = 1$ and $f_c = 0$. These factors are determined with the geometry shown in Figures 9 and 10 by using knife-edge diffraction considerations as follows:

$$\theta_{ce} = \text{Tan}^{-1}(2 h_{fc}/d_c) \quad \text{rad} \tag{130}$$

where h_{fc} is the height of the facility antenna above its counterpoise from (22), and d_c is the counterpoise diameter which is an IF-77 model input parameter [20, p. 88].

$$r_c = 0.5\, d_c/\cos\theta_{ce} \quad \text{km} \tag{131}$$

$$\theta_{kg} = |\theta_{ce}| - |\theta_{rl}| \quad \text{rad} \tag{132}$$

where θ_{rl} is from (116):

$$Y_v = \sqrt{\pi k r_c A} \tag{133}$$

where A is from (10b).

$$\theta_{kc} = \theta_{ce} - \theta_{hl} \quad \text{rad} \tag{134}$$

where θ_{hl} is calculated using counterpoise parameters in (106) through (118).

$$V_g = \pm Y_v \sin(\theta_{kg}/2) \begin{pmatrix} - & \text{for } |\theta_{rl}| < \theta_{ce} \\ + & \text{otherwise} \end{pmatrix} \tag{135a}$$

$$V_c = \pm Y_v \sin(\theta_{kc}/2) \begin{pmatrix} & \text{for } \theta_{hl} > \theta \\ & \text{otherwise} \end{pmatrix} \tag{135b}$$

5.2.3 Counterpoise Factors

Counterpoise factor, f_g, in (119a) is used to provide some reduction in the reflection from the earth's surface when this reflecting surface is shadowed by the counterpoise. Counterpoise factor, f_c, in (119b) is used to provide some reduction in the reflection from the counterpoise because of the limited area of the counterpoise. When there is no counterpoise, $f_g = 1$ and $f_c = 0$. These factors are determined with the geometry shown in Figures 9 and 10 by using knife-edge diffraction considerations as follows:

$$\theta_{ce} = \text{Tan}^{-1}(2\, h_{fc}/d_c) \quad \text{rad} \tag{130}$$

where h_{fc} is the height of the facility antenna above its counterpoise from (22), and d_c is the counterpoise diameter which is an ITS-77 model input parameter [20, p. 88].

$$r_c = 0.5\, d_c/\cos\theta_{ce} \quad \text{km} \tag{131}$$

$$\theta_{kg} = |\theta_{ce}| - |\theta_{rl}| \quad \text{rad} \tag{132}$$

where θ_{rl} is from (116):

$$Y_v = \sqrt{\pi r_c A} \tag{133}$$

where A is from (10b).

$$\theta_{kc} = \theta_{ce} - \theta_{hl} \quad \text{rad} \tag{134}$$

where θ_{hl} is calculated using counterpoise parameters in (106) through (118).

$$v_g = \pm\, Y_v \sin(\theta_{kg}/2) \begin{cases} - & \text{for } |\theta_{rl}| < \theta_{ce} \\ + & \text{otherwise} \end{cases} \tag{135a}$$

$$v_c = \pm\, Y_v \sin(\theta_{kc}/2) \begin{cases} & \text{for } \theta_{hl} > \theta \\ & \text{otherwise} \end{cases} \tag{135b}$$

$$C_{g,c} = \int_0^{v_{g,c}} \cos\left(\frac{\pi t^2}{2}\right) dt \ , \ S_{g,c} = \int_0^{v_{g,c}} \sin\left(\frac{\pi t^2}{2}\right) dt \qquad (136)$$

where these are Fresnel integrals [34, p. II 1-18].

$$f_{g,c} = 0.5\sqrt{[1 - (C_{g,c} + S_{g,c})]^2 + [(C_{g,c} - S_{g,c})]^2} \qquad (137)$$

$$\phi_{kg,c} = \mathrm{Tan}^{-1}\left(\frac{C_{g,c} - S_{g,c}}{C_{g,c} - S_{g,c}}\right) \ \mathrm{rad} \qquad (138)$$

The angles $\phi_{kg,c}$ are phase shifts that will be used later in Section 5.4.

5.2.4 Antenna Pattern Gain Factors

The antenna gain factors $g_{D,R}$ and $g_{Rh,v}$ are used to allow for situations where the antenna gains effective for the direct ray path differ from those for the reflected ray path. Figure 11 illustrates the two-ray path and indicates the gains

$\theta_{eH1,2}$ and $\theta_{g1,2}$ are measured from the horizontal at each terminal. Angles above the horizontal are positive.

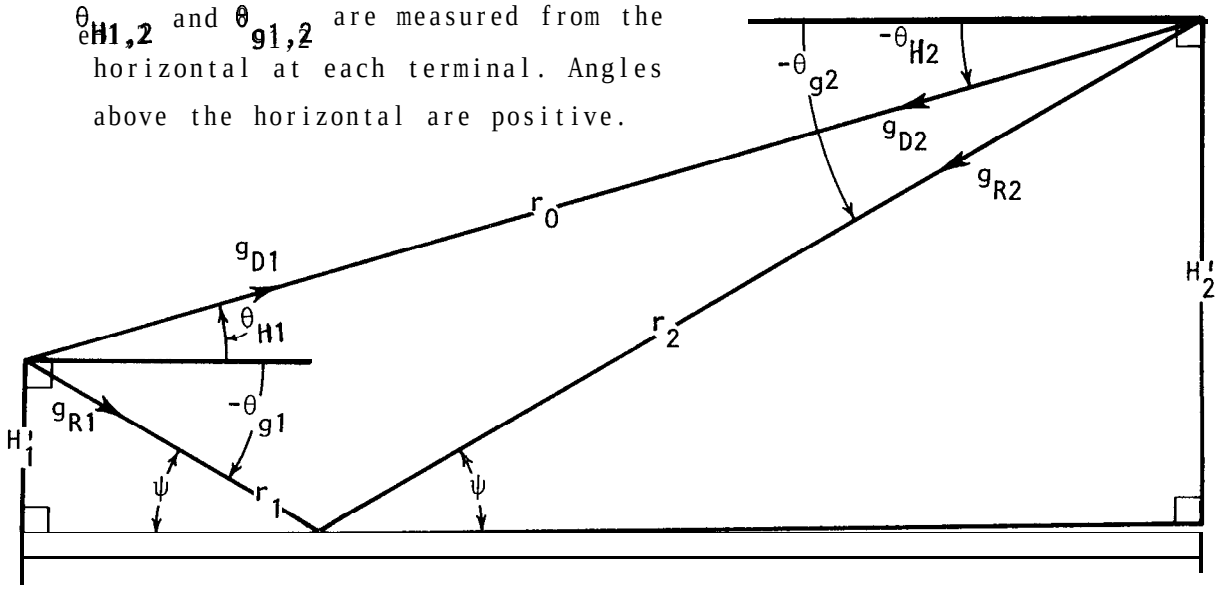

Note: This sketch is drawn with flat earth, straight rays and an exaggerated scale so that the geometry shown is over simplified.

FIGURE 11. SKETCH ILLUSTRATING ANTENNA GAIN NOTATION AND CORRESPONDENCE BETWEEN RAY TAKE-OFF ANGLES AND GAINS.

$$C_{g,c} = \int_0^{v_{g,c}} \cos\left(\frac{\pi t^2}{2}\right) dt \ , \ S_{g,c} = \int_0^{v_{g,c}} \sin\left(\frac{\pi t^2}{2}\right) dt \qquad (136)$$

where these are Fresnel integrals [34, p. II 1-18].

$$f_{g,c} = 0.5\sqrt{[1 - (C_{g,c} + S_{g,c})]^2 + ((C_{g,c} - S_{g,c}))^2} \qquad (137)$$

$$\phi_{kg,c} = \mathrm{Tan}^{-1}\left(\frac{C_{g,c} - S_{g,c}}{C_{g,c} - S_{g,c}}\right) \ \mathrm{rad} \qquad (138)$$

The angles $\phi_{kg,c}$ are phase shifts that will be used later in Section 5.4.

5.2.4 Antenna Pattern Gain Factors

The antenna gain factors $g_{D,R}$ and $g_{Rh,v}$ are used to allow for situations where the antenna gains effective for the direct ray path differ from those for the reflected ray path. Figure 11 illustrates the two-ray path and indicates the gains

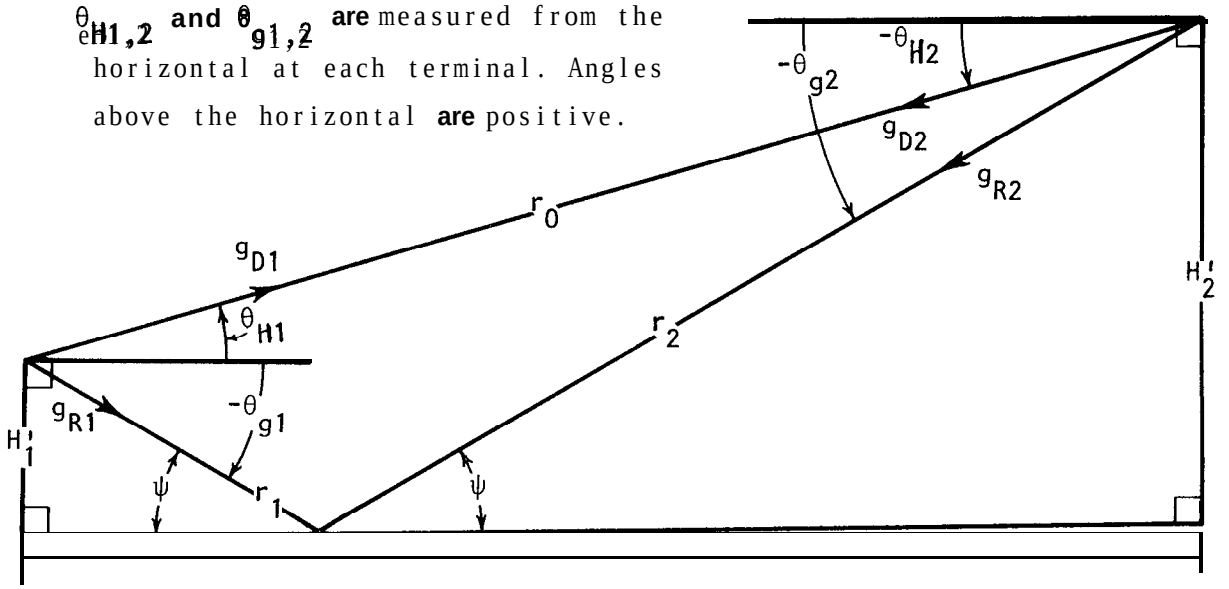

Note: This sketch is drawn with flat earth, straight rays and an exaggerated scale so that the geometry shown is over simplified.

FIGURE 11. SKETCH ILLUSTRATING ANTENNA GAIN NOTATION AND CORRESPONDENCE BETWEEN RAY TAKE-OFF ANGLES AND GAINS.

where isotropic implies that, for the radiation angles of interest, $g_{R1} = g_{D1}$ and $g_{R2} = g_{D2}$. In problems involving elliptical polarization, horizontally polarized ($g_{hD1,2}$ and $g_{hR1,2}$) and vertically polarized ($g_{vD1,2}$ and $g_{vR1,2}$) components are used. Linear polarization is considered to be either vertical or horizontal with the polarization associated with $g_{D,R}$ selected accordingly. Defining g_R as 1 for elliptical polarization is done to allow the antenna gains to be included in the reflection coefficient formulation of IF-77 in a simple way for horizontal or vertical polarization. Circular polarization is a special case of elliptical polarization; i.e.,

$$g_{hD1,2} = g_{vD1,2}$$

The gain factor g_{RV} is similar to g_R except that g_{RV} involves gains $g_{vR1,2}$; i.e.:

$$g_{RV}[V/V] = \begin{cases} 1 \text{ for isotropic antennas} \\ g_{vR1}g_{vR2} \quad \text{otherwise} \end{cases} \tag{143}$$

In a similar manner,

$$g_{Rh}[V/V] = \begin{cases} 1 \text{ for isotropic antennas} \\ g_{hR1}g_{hR2} \quad \text{otherwise} \end{cases} \tag{144}$$

where g_{Rh} is for horizontal polarization. These factors will be used in the formulation of complex plane-earth reflection coefficients for elliptical polarization that is given in the next section.

Several facility antenna patterns from which gain factors can be determined are included in the computer programs that utilize IF-77 [20, p. 85]. However, data for other facility antenna patterns or aircraft antenna patterns can be used. These programs also include an option to tilt the main beam of either or both antenna(s) relative to the horizontal, or have either or both antenna(s) track the other with its main beam [20, p. 89]. The patterns involved here are vertical plane antenna patterns. Gain variations with azimuth can be accommodated by adjusting $G_{T,R}$ in (4), and $G_{NT,R}$ for (4) are obtained from:

where isotropic implies that, for the radiation angles of interest, $g_{R1} = g_{D1}$ and $g_{R2} = g_{D2}$. In problems involving elliptical polarization, horizontally polarized ($g_{hD1,2}$ and $g_{hR1,2}$) and vertically polarized ($g_{vD1,2}$ and $g_{vR1,2}$) components are used. Linear polarization is considered to be either vertical or horizontal with the polarization associated with $g_{D,R}$ selected accordingly. Defining g_R as 1 for elliptical polarization is done to allow the antenna gains to be included in the reflection coefficient formulation of IF-77 in a simple way for horizontal or vertical polarization. Circular polarization is a special case of elliptical polarization; i.e.,

$$g_{hD1,2} = g_{vD1,2}$$

The gain factor g_{RV} is similar to g_R except that g_{RV} involves gains $g_{vR1,2}$; i.e.:

$$g_{RV}[V/V] = \begin{cases} 1 \text{ for isotropic antennas} \\ g_{vR1}g_{vR2} \quad \text{otherwise} \end{cases} \tag{143}$$

In a similar manner,

$$g_{Rh}[V/V] = \begin{cases} 1 \text{ for isotropic antennas} \\ g_{hR1}g_{hR2} \quad \text{otherwise} \end{cases} \tag{144}$$

where g_{Rh} is for horizontal polarization. These factors will be used in the formulation of complex plane-earth reflection coefficients for elliptical polarization that is given in the next section.

Several facility antenna patterns from which gain factors can be determined are included in the computer programs that utilize IF-77 [20, p. 85]. However, data for other facility antenna patterns or aircraft antenna patterns can be used. These programs also include an option to tilt the main beam of either or both antenna(s) relative to the horizontal, or have either or both antenna(s) track the other with its main beam [20, p. 89]. The patterns involved here are vertical plane antenna patterns. Gain variations with azimuth can be accommodated by adjusting $G_{T,R}$ in (4), and $G_{NT,R}$ for (4) are obtained from:

When a counterpoise is present, it will have a set of gain factors associated with it where the earth or counterpoise set values are determined by the values used for $H_{1,2}$ in (106) to calculate $\theta_{h1,2}$ and $\theta_{r1,2}$. For example:

$$g_{Rg} = g_R \text{ calculated with parameters appropriate for a ground reflection} \quad (149a)$$

$$g_{Rc} = g_R \text{ calculated with parameters appropriate for a counterpoise reflection} \quad (149b)$$

5.2.5 Plane-Earth Reflection Coefficients

Values for the plane-earth reflection coefficient, $R \exp(-j\phi)$, are dependent upon the dielectric constant, E, and conductivity, CT, of the surface involved. For water:

$$\varepsilon = \frac{\varepsilon_s - \varepsilon_0}{1 + (2\pi fT)^2} + \varepsilon_0 \quad (150)$$

$$\sigma[\text{mho/m}] = \frac{f^2 T(\varepsilon - \varepsilon_0)}{2865} + \sigma_i \quad (151)$$

where ε_s is the static dielectric constant, $\varepsilon_0 = 4.9$ is the dielectric constant representing the sum of electronic and atomic polarizations, f[MHz] is frequency, T[μs] is relaxation time, and σ_i[mho/m] is the ionic conductivity. The values for ε_s, T, and σ_i for water [15, p. 26] were obtained using Saxton and Lane [36]. When (150, 151) are not used, appropriate ε and σ values are taken from the Applications Guide [20, p. 89]. The formulation for $R \exp(-j\phi)$ may be summarized as follows:

$$\varepsilon_c = \varepsilon - j\, 60\, \lambda_m\, \sigma \quad (152)$$

where λ_m is from (10a).

$$\gamma_c = \sqrt{k\varepsilon_c - \cos^2\psi} \quad (153)$$

When a counterpoise is present, it will have a set of gain factors associated with it where the earth or counterpoise set values are determined by the values used for $H_{1,2}$ in (106) to calculate $\theta_{h1,2}$ and $\theta_{r1,2}$. For example:

$$g_{Rg} = g_R \text{ calculated with parameters appropriate for a ground reflection} \tag{149a}$$

$$g_{Rc} = g_R \text{ calculated with parameters appropriate for a counterpoise reflection} \tag{149b}$$

5.2.5 Plane-Earth Reflection Coefficients

Values for the plane-earth reflection coefficient, $R \exp(-j\phi)$, are dependent upon the dielectric constant, ε, and conductivity, σ, of the surface involved. For water:

$$\varepsilon = \frac{\varepsilon_s - \varepsilon_0}{1 + (2\pi fT)^2} + \varepsilon_0 \tag{150}$$

$$\sigma[\text{mho/m}] = \frac{f^2 T(\varepsilon - \varepsilon_0)}{2865} + \sigma_i \tag{151}$$

where ε_s is the static dielectric constant, $\varepsilon_0 = 4.9$ is the dielectric constant representing the sum of electronic and atomic polarizations, f[MHz] is frequency, T[μs] is relaxation time, and σ_i[mho/m] is the ionic conductivity. The values for ε_s, T, and σ_i for water [15, p. 26] were obtained using Saxton and Lane [36]. When (150, 151) are not used, appropriate ε and σ values are taken from the Applications Guide [20, p. 89]. The formulation for $R \exp(-j\phi)$ may be summarized as follows:

$$\varepsilon_c = \varepsilon - j\ 60\ \lambda_m\ \sigma \tag{152}$$

where λ_m is from (10a).

$$\gamma_c = j k \sqrt{\varepsilon_c - \cos^2 \psi} \tag{153}$$

where the geometry used in calculating gain factors (Sec. 5.2.4) is dependent on the use of $H_{1,2}$ values in (106) that are appropriate for either ground or counterpoise reflection.

The total phase lag of the reflected ray relative to the direct ray for ground, ϕ_{Tg}, or counterpoise, ϕ_{Tc}, is given by:

$$\phi_{g,c} = (2\pi Arg_{g,c}/\lambda) + \phi_{g,c} + \phi_{kg,c} + \phi_{g,c}^2/2 \quad \text{rad} \tag{157}$$

where $Arg_{g,c}$ is from (114), A is from (10b), $\phi_{kg,c}$ is from (138), and $v_{g,c}$ is from (135). If there is no counterpoise, the last two terms of (157) may be neglected since they are the phase lag introduced by knife-edge diffraction over the counterpoise.

5.3 Line-of-Sight Transition Distance, d_0

The largest distance in the line-of-sight region at which diffraction is considered negligible is d_0. In the IF-73 model, it was estimated using the distance at which the attenuation associated with a modified diffraction line is zero [14, p. 66]. The IF-73 d_0 is called d_d and in the IF-77 model is calculated as follows:

$$\theta_{h5} = 2 \text{ Sin}^{-1}\left[\left(\frac{0.5}{5.1658}\right)\sqrt{d_{ML}/[fd_{L1}(d_{ML}-d_{L1})]}\right] \quad \text{rad} \tag{158}$$

where d_{ML} is from (43), f[MHz] is frequency, and d_{L1} is from Figure 5:

$$\theta_5 = \theta_{h5} - \text{Tan}^{-1}\{[(h_1 - h_{L1})/d_{L1}] - d_{L1}/2a\} \tag{159}$$

where h_{L1} is from Figure 5, h_1 is from (21), and a is from 16.

$$h_{em2} = h_2 - \Delta h_{e2} \quad \text{km} \tag{160}$$

where h_2 is the aircraft altitude above msl (Fig. 2), and Δh_{e2} is from (25).

where the geometry used in calculating gain factors (Sec. 5.2.4) is dependent on the use of $H_{1,2}$ values in (106) that are appropriate for either ground or counterpoise reflection.

The total phase lag of the reflected ray relative to the direct ray for ground, ϕ_{Tg}, or counterpoise, ϕ_{Tc}, is given by:

$$\phi_{g,c} = (2\pi Arg_{g,c}/\lambda) + \phi_{g,c} + \phi_{kg,c} + \phi_{g,c}^2/2 \quad \text{rad} \tag{157}$$

where $Arg_{g,c}$ is from (114), A is from (10b), $\phi_{kg,c}$ is from (138), and $v_{g,c}$ is from (135). If there is no counterpoise, the last two terms of (157) may be neglected since they are the phase lag introduced by knife-edge diffraction over the counterpoise.

5.3 Line-of-Sight Transition Distance, d_0

The largest distance in the line-of-sight region at which diffraction is considered negligible is d_0. In the IF-73 model, it was estimated using the distance at which the attenuation associated with a modified diffraction line is zero [14, p. 66]. The IF-73 d_0 is called d_d and in the IF-77 model is calculated as follows:

$$\theta_{h5} = 2 \text{ Sin}^{-1}\left[\left(\frac{0.5}{5.1658}\right)\sqrt{d_{ML}/[fd_{L1}(d_{ML}-d_{L1})]}\right] \quad \text{rad} \tag{158}$$

where d_{ML} is from (43), f[MHz] is frequency, and d_{L1} is from Figure 5:

$$\theta_5 = \theta_{h5} - \text{Tan}^{-1}\{[(h_1 - h_{L1})/d_{L1}] - d_{L1}/2a\} \tag{159}$$

where h_{L1} is from Figure 5, h_1 is from (21), and a is from 16.

$$h_{em2} = h_2 - \Delta h_{e2} \quad \text{km} \tag{160}$$

where h_2 is the aircraft altitude above msl (Fig. 2), and Δh_{e2} is from (25).

where W is from (94), and

$$d_d = d_{ML} + A_{ML}(d_{ML} - d_5) / (A_{ML} - A_5) \quad \text{km} \tag{171}$$

where A_{ML} is from (95) and d_{ML} from (43).

Values estimated for d_0 in IF-73 have been found to be too small when low antennas are used for both antennas. To correct this difficulty, d_0 estimates in IF-77 are made using:

$$d_0 = \left\{ \begin{array}{l} d_{L1} \text{ when } d_{L1} > d_d \\ d_{\lambda/6} \text{ when } d_{\lambda/6} > d_{L1} \text{ and } d_d \\ d_d \quad \text{otherwise} \end{array} \right\} \quad \text{km}$$

where d_{L1} is the horizon distance for the lower terminal (Fig. 5); $d_{\lambda/6}$ is the distance at which the path length difference, Δr, in a two-ray line-of-sight formulation is equal to $\lambda/6$ (λ is wave length); and d_d is the d_0 of IF-73 [14, p. 66]. The distance $d_{\lambda/6}$ is the largest distance at which a free-space value is obtained in a two-ray model of reflection from a smooth earth with a reflection coefficient of -1. A value for $d_{\lambda/6}$ can be determined by the repetitive use of the line-of-sight formulation (Sec. 5.1) to define the Δr to distance relationship; i.e., (102) through (118).

5.4 Line-of-Sight Attenuation, A_{LOS}

Line-of-sight attenuation, A_{LOS}, is calculated as follows:

$$F_{fs} = \left\{ \begin{array}{l} 1 \text{ if lobing option is used and } \Delta r_g < 10\lambda \\ 1 \text{ if } \Delta r_g \leq 0.5\lambda \quad \text{and} \\ \quad | g_D + R_{Tg} \exp(-j\phi_{Tg}) | \leq g_D \\ 0 \quad \text{otherwise} \end{array} \right\} \tag{173}$$

where Δr_g is from (114), λ is from (10a), g_D is obtained using earth reflection geometry as indicated in Section 5.2.4, and $R_{Tg} \angle \exp(-j\phi_{Tg})$ is from (119, 157).

where W is from (94), and

$$d_d = d_{ML} + A_{ML}(d_{ML} - d_5) / (A_{ML} - A_5) \quad \text{km} \tag{171}$$

where A_{ML} is from (95) and d_{ML} from (43).

Values estimated for d_0 in IF-73 have been found to be too small when low antennas are used for both antennas. To correct this difficulty, d_0 estimates in IF-77 are made using:

$$d_0 = \left\{ \begin{array}{l} d_{L1} \text{ when } d_{L1} > d_d \\ d_{\lambda/6} \text{ when } d_{\lambda/6} > d_{L1} \text{ and } d_d \\ d_d \quad \text{otherwise} \end{array} \right\} \quad \text{km}$$

where d_{L1} is the horizon distance for the lower terminal (Fig. 5); $d_{\lambda/6}$ is the distance at which the path length difference, Δr, in a two-ray line-of-sight formulation is equal to $\lambda/6$ (λ is wave length); and d_d is the d_0 of IF-73 [14, p. 66]. The distance $d_{\lambda/6}$ is the largest distance at which a free-space value is obtained in a two-ray model of reflection from a smooth earth with a reflection coefficient of -1. A value for $d_{\lambda/6}$ can be determined by the repetitive use of the line-of-sight formulation (Sec. 5.1) to define the Δr to distance relationship; i.e., (102) through (118).

5.4 Line-of-Sight Attenuation, A_{LOS}

Line-of-sight attenuation, A_{LOS}, is calculated as follows:

$$F_{fs} = \left\{ \begin{array}{l} 1 \text{ if lobing option is used and } \Delta r_g < 10\lambda \\ 1 \text{ if } \Delta r_g \leq 0.5\lambda \quad \text{and} \\ \quad | g_D + R_{Tg} \exp(-j\phi_{Tg}) | \leq g_D \\ 0 \quad \text{otherwise} \end{array} \right\} \tag{173}$$

where Δr_g is from (114), λ is from (10a), g_D is obtained using earth reflection geometry as indicated in Section 5.2.4, and $R_{Tg} \angle \exp(-j\phi_{Tg})$ is from (119, 157).

where $h_{Lr1,2}$ is from (39, 47), a is from (16), the effective reflection surface elevation, h_r, is an input parameter, and $d_{L1,2}$ is from (41, 46).

$$d_s = d - d_{L1} - d_{L2} \quad \text{km} \tag{179}$$

where the great circle path distance, d, may be taken as an input parameter.

$$\theta_s = \theta_{a1} + \theta_{a2} + d_s/a \quad \text{rad} \tag{180}$$

$$d_{z1} = \left[\left(\frac{d_s}{2a} + \theta_{a2}\right) d_s + h_{L2} - h_{L1}\right] / \theta_s \quad \text{km} \tag{181}$$

where $h_{L1,2}$ are from (38, 48).

$$d_{z2} = d_s - d_{z1} \quad \text{km} \tag{182}$$

$$A_m = 157 \ (10^{-6}) \ \text{per km} \tag{183}$$

$$dN = A_m - a^{-1} \quad \text{per km} \tag{184}$$

$$\gamma_e = N_s \ (10^{-6})/dN \quad \text{km} \tag{185}$$

where N_s is from (14).

$$z_{a1,2} = \frac{1}{2a}\left(\frac{d_{z1,2}}{2}\right)^2 + \theta_{a1,2}\left(\frac{d_{z1,2}}{2}\right) + h_{Lr1,2} \quad \text{km} \tag{186}$$

$$z_{b1,2} = \frac{1}{2a} d_{z1,2}^2 + \theta_{a1,2}\, d_{z1,2} + h_{Lr1,2} \quad \text{km} \tag{187}$$

$$\theta_{o1,2} = A_m - dN \exp(-h_{Lr1,2}/\gamma_e) \tag{188}$$

$$\theta_{a1,2} = A_m - dN \exp(-z_{a1,2}/\gamma_e) \tag{189}$$

where $h_{Lr1,2}$ is from (39, 47), a is from (16), the effective reflection surface elevation, h_r, is an input parameter, and $d_{L1,2}$ is from (41, 46).

$$d_s = d - d_{L1} - d_{L2} \quad \text{km} \tag{179}$$

where the great circle path distance, d, may be taken as an input parameter.

$$\theta_s = \theta_{a1} + \theta_{a2} + d_s/a \quad \text{rad} \tag{180}$$

$$d_{z1} = \left[\left(\frac{d_s}{2a} + \theta_{a2}\right) d_s + h_{L2} - h_{L1}\right] / \theta_s \quad \text{km} \tag{181}$$

where $h_{L1,2}$ are from (38, 48).

$$d_{z2} = d_s - d_{z1} \quad \text{km} \tag{182}$$

$$A_m = 157 \ (10^{-6}) \ \text{per km} \tag{183}$$

$$dN = A_m - a^{-1} \quad \text{per km} \tag{184}$$

$$\gamma_e = N_s \ (10^{-6})/dN \quad \text{km} \tag{185}$$

where N_s is from (14).

$$z_{a1,2} = \frac{1}{2a}\left(\frac{d_{z1,2}}{2}\right)^2 + \theta_{a1,2}\left(\frac{d_{z1,2}}{2}\right) + h_{Lr1,2} \quad \text{km} \tag{186}$$

$$z_{b1,2} = \frac{1}{2a} d_{z1,2}^2 + \theta_{a1,2}\, d_{z1,2} + h_{Lr1,2} \quad \text{km} \tag{187}$$

$$\theta_{o1,2} = A_m - dN \exp(-h_{Lr1,2}/\gamma_e) \tag{188}$$

$$\theta_{a1,2} = A_m - dN \exp(-z_{a1,2}/\gamma_e) \tag{189}$$

where $h_{Lr1,2}$ is from (39, 47), a is from (16), the effective reflection surface elevation, h_r, is an input parameter, and $d_{L1,2}$ is from (41, 46).

$$d_s = d - d_{L1} - d_{L2} \quad \text{km} \tag{179}$$

where the great circle path distance, d, may be taken as an input parameter.

$$\theta_s = \theta_{a1} + \theta_{a2} + d_s/a \quad \text{rad} \tag{180}$$

$$d_{z1} = \left[\left(\frac{d_s}{2a} + \theta_{a2}\right) d_s + h_{L2} - h_{L1}\right] \Big/ \theta_s \quad \text{km} \tag{181}$$

where $h_{L1,2}$ are from (38, 48).

$$d_{z2} = d_s - d_{z1} \quad \text{km} \tag{182}$$

$$A_m = 157 \ (10^{-6}) \text{ per km} \tag{183}$$

$$dN = A_m - a^{-1} \text{ per km} \tag{184}$$

$$\gamma_e = N_s \ (10^{-6})/dN \quad \text{km} \tag{185}$$

where N_s is from (14).

$$z_{a1,2} = \frac{1}{2a}\left(\frac{d_{z1,2}}{2}\right)^2 + \theta_{a1,2}\left(\frac{d_{z1,2}}{2}\right) + h_{Lr1,2} \quad \text{km} \tag{186}$$

$$z_{b1,2} = \frac{1}{2a} d_{z1,2}^2 + \theta_{a1,2}\, d_{z1,2} + h_{Lr1,2} \quad \text{km} \tag{187}$$

$$\theta_{o1,2} = A_m - dN \exp(-h_{Lr1,2}/\gamma_e) \tag{188}$$

$$\theta_{a1,2} = A_m - dN \exp(-z_{a1,2}/\gamma_e) \tag{189}$$

$$K = 2\pi/\lambda \quad \text{per km} \tag{214}$$

where K is the wave number and λ is from (10b).

$$\rho_{1,2} = 2K\theta h_{e1,2} \tag{215}$$

where $h_{e1,2}$ are from (24).

$$q_{1,2} = \chi^2_{v1,2} + \rho^2_{1,2} \tag{216}$$

$$B_{BS} = 6 + 8s^2 + 8(1+s)\chi^2_{v2}\rho^2_2/q^2_2 + 8(1-s)\chi^2_{v1}\rho^2_1/q^2_1 + 2((1-s^2)(1+2\chi^2_{v1}/q_1)(1+2\chi^2_{v2}/q_2) \tag{217}$$

$$C_s = 12\left(\frac{\rho_1+\sqrt{2}}{\rho_1}\right)^2\left(\frac{\rho_2+\sqrt{2}}{\rho_2}\right)^2\left(\frac{\rho_1+\rho_2}{\rho_1+\rho_2+2\sqrt{2}}\right) \tag{218}$$

$$S_V = 10\log\left(\frac{(A\eta^2 + B_s\eta)q_1q_2}{\rho_1^2\rho_2^2} + C_s\right) \quad \text{dB} \tag{219}$$

where S_V is the scattering volume term, and

$$A_s = S_e + S_V + 10\log(K\theta^3/\lambda d) \quad \text{dB} \tag{220}$$

where As is the tropospheric scatter attenuation.

$$K = 2\pi/\lambda \quad \text{per km} \tag{214}$$

where K is the wave number and λ is from (10b).

$$\rho_{1,2} = 2K\theta h_{e1,2} \tag{215}$$

where $h_{e1,2}$ are from (24).

$$q_{1,2} = \chi^2_{v1,2} + \rho^2_{1,2} \tag{216}$$

$$B_{BS} = 6 + 8s^2 + 8(1+s)\chi^2_{v2}\rho^2_2/q^2_2 + 8(1-s)\chi^2_{v1}\rho^2_1/q^2_1 + 2((1-s^2)(1+2\chi^2_{v1}/q_1)(1+2\chi^2_{v2}/q_2) \tag{217}$$

$$C_s = 12\left(\frac{\rho_1+\sqrt{2}}{\rho_1}\right)^2\left(\frac{\rho_2+\sqrt{2}}{\rho_2}\right)^2\left(\frac{\rho_1+\rho_2}{\rho_1+\rho_2+2\sqrt{2}}\right) \tag{218}$$

$$S_V = 10\log\left(\frac{(A\eta^2 + B_s\eta)q_1q_2}{\rho_1^2\rho_2^2} + C_s\right) \quad \text{dB} \tag{219}$$

where S_V is the scattering volume term, and

$$A_s = S_e + S_V + 10\log(K\theta^3/4) \quad \text{dB} \tag{220}$$

where As is the tropospheric scatter attenuation.

where $h_{L1,2}$ are from (38,48)

$$r_{BH} = r_{L1} + r_{L2} + d_s \quad \text{km} \tag{224}$$

where d_s is from (179)

$$r = \text{greater of} \begin{Bmatrix} r_o \text{ or } r_{WH} \text{ for LOS} \\ \text{or} \\ d \text{ or } r_{BH} \text{ otherwise} \end{Bmatrix} \quad \text{km} \tag{225}$$

where r_o is from (112), and

$$L_{bf} = 32.45 + 20 \log (fr) \quad \text{dB} \tag{226}$$

where frequency, f[MHz], is a starting parameter [20, p. 82].

9. ATMOSPHERIC ABSORPTION

The formulation used to estimate median values for atmospheric absorption is similar to the IF-73 method [14, Sec. A.4.5]. Allowances are made for absorption due to oxygen and water vapor by using surface absorption rates and effective ray lengths where these ray lengths are lengths contained within atmospheric layers with appropriate effective thicknesses. Geometry associated with this formulation is shown in Figure 12 along with key equations relating geometric parameters. This geometry is used to calculate effective ray lengths applicable to the oxygen, r_{eo}, rain storm, r_{es} for Section 10.4, and water vapor, r_{ew}, layers for different path configurations. The rain storm is assumed to occur between the facility and its maximum LOS distance, d_{ML} from (43), so that only the facility horizon ray is considered in the calculation of r_{es} for beyond-the-horizon paths.

For line-of-sight paths, $(d \geq d_{ML})$ where d is a specified parameter except in the LOS region where it is calculated using (118), d_{ML} is from (43), the Figure 12 expressions are used to calculate effective ray lengths, r_{eo}'s with $H_{y1,2} = H_{1,2}$ from (106), for earth, $a_y = a_a$ from (104), and $\beta = \theta_{h1}$ from (115a).

where $h_{L1,2}$ are from (38,48)

$$r_{BH} = r_{L1} + r_{L2} + d_s \quad \text{km} \tag{224}$$

where d_s is from (179)

$$r = \text{greater of} \begin{Bmatrix} r_o \text{ or } r_{WH} \text{ for LOS} \\ \text{or} \\ d \text{ or } r_{BH} \text{ otherwise} \end{Bmatrix} \quad \text{km} \tag{225}$$

where r_o is from (112), and

$$L_{bf} = 32.45 + 20 \log (fr) \quad \text{dB} \tag{226}$$

where frequency, f[MHz], is a starting parameter [20, p. 82].

9. ATMOSPHERIC ABSORPTION

The formulation used to estimate median values for atmospheric absorption is similar to the IF-73 method [14, Sec. A.4.5]. Allowances are made for absorption due to oxygen and water vapor by using surface absorption rates and effective ray lengths where these ray lengths are lengths contained within atmospheric layers with appropriate effective thicknesses. Geometry associated with this formulation is shown in Figure 12 along with key equations relating geometric parameters. This geometry is used to calculate effective ray lengths applicable to the oxygen, r_{eo}, rain storm, r_{es} for Section 10.4, and water vapor, r_{ew}, layers for different path configurations. The rain storm is assumed to occur between the facility and its maximum LOS distance, d_{ML} from (43), so that only the facility horizon ray is considered in the calculation of r_{es} for beyond-the-horizon paths.

For line-of-sight paths, $(d \geq d_{ML})$ where d is a specified parameter except in the LOS region where it is calculated using (118), d_{ML} is from (43), the Figure 12 expressions are used to calculate effective ray lengths, r_{eo}'s with $H_{y1,2} = H_{1,2}$ from (106), for earth, $a_y = a_a$ from (104), and $\beta = \theta_{h1}$ from (115a).

For single horizon paths, ($d_{ML} < d \leq d_{L1} + d_{Lo1}$) where d_{L1} is from Figure 5 and d_{Lo1} is from (52), the Figure 12 expressions are used with one (R_{es}) or two ($R_{eo,w}$) sets of starting parameters and the $R_{eo,s,w}$'s obtained with these are called $r_{1eo,s,w}$ and $r_{2eo,w}$. In the calculation of $r_{1eo,s,w}$, H_{y1} = lesser of (h_{e1} or h_{Lr1}) and H_{y2} = greater of (h_{e1} or h_{Lr1}) where h_{e1} is from (24) and h_{Lr1} is from (39); a_y = a from (16) and $\beta = \theta_{e1}$ from (40) if $H_{y1} = h_{e1}$, otherwise $\beta = \theta_L$ from (42). In calculation for $r_{2eo,w}$, H_{y1} = lesser of (h_{e2} from (24) or h_{Lr1})) and H_{y2} = greater of (h_{e2} or h_{Lr2}) with $\beta = \theta_{e2}$ from (49) if $H_{y1} = h_{e2}$, otherwise $\beta = -\theta_L$. Values for $r_{eo,s,w}$ are then obtained using:

$$r_{es} = r_{1es} \quad \text{km} \tag{227a}$$

$$r_{eo,w} = r_{1eo,w} + r_{2eo,w} \quad \text{km} \tag{227b}$$

For two-horizon paths ($d_{L1} + d_{Lo1} < d$), the Figure 12 expressions are also used with one (R_{es}) or two ($R_{eo,w}$) sets of input parameters. The results obtained are called $r_{1eo,s,w}$ and $r_{2eo,s,w}$, where (227) is used to determine $r_{eo,s,w}$ values. In calculations for $r_{1eo,s,w}$, H_{y1} = lesser of {h_{e1} or h_v from (201)}, H_{y2} = greater of {h_{e1} or h_v}, $\beta = \theta_{e1}$ if $H_{y1} = h_{e1}$, otherwise $\beta = -\text{Tan}^{-1}\theta_{A1}$ where θ_{A1} is from (196). In calculations for $r_{2eo,s,w}$, H_{y1} = lesser of {h_v or h_{e2}}, H_{y2} = greater of {h_v or h_{e2}}, a_y = a and $\beta = \theta_{e2}$ if $H_{y1} = h_{e2}$, otherwise $\beta = -\text{Tan}^{-1}\theta_{A2}$, where θ_{A2} is from (196).

Surface absorption rates for oxygen and water vapor, $\gamma_{oo,w}$ are used with effective ray lengths, $r_{eo,w}$ to obtain an estimate for atmospheric absorption, A,; i.e.,:

$$A, = \gamma_{oo}\, r_{eo} + \gamma_{ow}\, r_{ew} \quad \frac{dB}{dB} \,, \tag{223}$$

Values for $\gamma_{oo,w}$ are obtained by interpolating between values taken from the Rice et al. curves [34, p. 3-7].

For single horizon paths, ($d_{ML} < d \leq d_{L1} + d_{Lo1}$) where d_{L1} is from Figure 5 and d_{Lo1} is from (52), the Figure 12 expressions are used with one (R_{es}) or two ($R_{eo,w}$) sets of starting parameters and the $R_{eo,s,w}$'s obtained with these are called $r_{leo,s,w}$ and $r_{2eo,w}$. In the calculation of $r_{leo,s,w}$, H_{y1} = lesser of (h_{e1} or h_{Lr1}) and H_{y2} = greater of (h_{e1} or h_{Lr1}) where h_{e1} is from (24) and h_{Lr1} is from (39); a_y = a from (16) and $\beta = \theta_{e1}$ from (40) if $H_{y1} = h_{e1}$, otherwise $\beta = \theta_L$ from (42). In calculation for $r_{2eo,w}$, H_{y1} = lesser of (h_{e2} from (24) or h_{Lr1})) and H_{y2} = greater of (h_{e2} or h_{Lr2}) with $\beta = \theta_{e2}$ from (49) if $H_{y1} = h_{e2}$, otherwise $\beta = -\theta_L$. Values for $r_{eo,s,w}$ are then obtained using:

$$r_{es} = r_{les} \quad \text{km} \tag{227a}$$

$$r_{eo,w} = r_{leo,w} + r_{2eo,w} \quad \text{km} \tag{227b}$$

For two-horizon paths ($d_{L1} + d_{Lo1} < d$), the Figure 12 expressions are also used with one (R_{es}) or two ($R_{eo,w}$) sets of input parameters. The results obtained are called $r_{leo,s,w}$ and $r_{2eo,s,w}$, where (227) is used to determine $r_{eo,s,w}$ values. In calculations for $r_{leo,s,w}$, H_{y1} = lesser of {h_{e1} or h_v from (201)}, H_{y2} = greater of {h_{e1} or h_v}, $\beta = \theta_{e1}$ if $H_{y1} = h_{e1}$, otherwise $\beta = -\text{Tan}^{-1}\theta_{A1}$ where θ_{A1} is from (196). In calculations for $r_{2eo,s,w}$, H_{y1} = lesser of {h_v or h_{e2}}, H_{y2} = greater of {h_v or h_{e2}}, a_y = a and $\beta = \theta_{e2}$ if $H_{y1} = h_{e2}$, otherwise $\beta = -\text{Tan}^{-1}\theta_{A2}$, where θ_{A2} is from (196).

Surface absorption rates for oxygen and water vapor, $\gamma_{oo,w}$ are used with effective ray lengths, $r_{eo,w}$ to obtain an estimate for atmospheric absorption, A,; i.e.,:

$$A, = \gamma_{oo}\, r_{eo} + \gamma_{ow}\, r_{ew} \quad \frac{dB}{dB} \,, \tag{223}$$

Values for $\gamma_{oo,w}$ are obtained by interpolating between values taken from the Rice et al. curves [34, p. 3-7].

where d_{Lq} is a total smooth earth horizon distance determined by ray tracing (Sec. 3) with $N_s = 329$ in (17) which would correspond to a 9000 km effective earth radius [34, p. 4-4]

$$d_e = \begin{cases} 130 d/d_q & \text{for } d \leq d_q \\ 130 + d - d_q & \text{otherwise} \end{cases} \quad \text{km} \tag{232}$$

where d is the great-circle path distance and is a specified parameter except in the LOS region where it is calculated via (118). Key parameters, g(0.1 or 0.9,f), V(0.5) and Y_0(0.1 or 0.9) for the long-term variability normally used are determined as follows:

$$g(0.1,f) = \begin{cases} 0.21 \sin[5.22 \log(f/200)] + 1.28 & \text{for } 60 \leq f \leq 1600 \text{ MHz} \\ 1.05 & \text{for } f > 1600 \text{ MHz} \end{cases} \tag{233a}$$

$$g(0.9,f) = \begin{cases} 0.18 \sin[5.22 \log(f/200)] + 1.23 & \text{for } 60 \leq f \leq 1600 \text{ MHz} \\ 1.05 & \text{for } f > 1600 \text{ MHz} \end{cases} \tag{233b}$$

$$f_2 = f_\infty + (f_m - f_\infty) \exp\left(-c_2 d_e^{n_2}\right) \tag{234}$$

and

$$\left.\begin{matrix} V(0.5) \\ Y_0(0.1) \\ -Y_0(0.9) \end{matrix}\right\} = \left[c_1 d_e^{n_1} - f_2\right] \exp\left(-c_3 d_e^{n_3}\right) + f_2 \text{ dB} \tag{235}$$

where the values used for the parameters c_1, c_2, c_3, n_1, n_2, n_3, f_m, and f_∞ depend on whether V(0.5) [34, Table III.5, Climate 1], Y(0.1) [34, Table III.3, all hours all year], or Y(0.9) [34, Table III.4, all hours all year] is calculated. This selection is based on a recommended model [11, p. 19] that was tested against air/ground data [10, Sec. 4.3]. However, other options such as different time blocks (Sec. 10.1.1), climates (Sec. 10.1.2), or a mix performed to meet particular

where d_{Lq} is a total smooth earth horizon distance determined by ray tracing (Sec. 3) with $N_s = 329$ in (17) which would correspond to a 9000 km effective earth radius [34, p. 4-4]

$$d_e = \begin{cases} 130 d/d_q & \text{for } d \leq d_q \\ 130 + d - d_q & \text{otherwise} \end{cases} \quad \text{km} \tag{232}$$

where d is the great-circle path distance and is a specified parameter except in the LOS region where it is calculated via (118). Key parameters, g(0.1 or 0.9,f), V(0.5) and Y_0(0.1 or 0.9) for the long-term variability normally used are determined as follows:

$$g(0.1,f) = \begin{cases} 0.21 \sin[5.22 \log(f/200)] + 1.28 & \text{for } 60 \leq f \leq 1600 \text{ MHz} \\ 1.05 & \text{for } f > 1600 \text{ MHz} \end{cases} \tag{233a}$$

$$g(0.9,f) = \begin{cases} 0.18 \sin[5.22 \log(f/200)] + 1.23 & \text{for } 60 \leq f \leq 1600 \text{ MHz} \\ 1.05 & \text{for } f > 1600 \text{ MHz} \end{cases} \tag{233b}$$

$$f_2 = f_\infty + (f_m - f_\infty) \exp\left(-c_2 d_e^{n_2}\right) \tag{234}$$

and

$$\left.\begin{matrix} V(0.5) \\ Y_0(0.1) \\ -Y_0(0.9) \end{matrix}\right\} = \left[c_1 d_e^{n_1} - f_2\right] \exp\left(-c_3 d_e^{n_3}\right) + f_2 \text{ dB} \tag{235}$$

where the values used for the parameters c_1, c_2, c_3, n_1, n_2, n_3, f_m, and f_∞ depend on whether V(0.5) [34, Table III.5, Climate 1], Y(0.1) [34, Table III.3, all hours all year], or Y(0.9) [34, Table III.4, all hours all year] is calculated. This selection is based on a recommended model [11, p. 19] that was tested against air/ground data [10, Sec. 4.3]. However, other options such as different time blocks (Sec. 10.1.1), climates (Sec. 10.1.2), or a mix performed to meet particular

$$A_y = \begin{cases} 0 \text{ if } A_{y1} \geq 0 \\ 10 \text{ if } A_{y1} \geq 10 \\ A_{y1} \text{ otherwise} \end{cases} \quad (243)$$

$$Y_e(q<0.1) = \begin{cases} \text{lesser of } [Y_{e1}(q) \text{ or } Y_T] \text{ for lobing} \\ \text{lesser of } [Y_{e1}(q) \text{ or } L_{br} + A_y \cdot (L_{bf} - c_y)] \\ \text{otherwise} \end{cases} \text{ dB} \quad (244)$$

where c_Y is 6, 5.8, and 5 dB for q values of 0.0001, 0.001, and 0.01, respectively,

$$Y_e(q>0.1) \equiv Y_{e1}(q) \text{ dB} . \quad (245)$$

10.1.1 Time Blocks

Long-term variability options for IF-77 include variabilities appropriate for the time blocks shown in Table 1 [20, p. 103]. These blocks and seasonal groupings are used to describe the diurnal and seasonal variations in a continental temperate climate [34, Sec. III.7.1]. They are incorporated into (235) by selecting appropriate constants from Rice et al. [34, Tables III.2, III.3, and III.4]. The expressions for $g(0.1,f)$ and $g(0.9,f)$ given in (233) are used for time block variabilities.

If a combination of time blocks is appropriate, various distributions can be mixed (Sec. 10.6).

10.1.2 Climates

Options to use various climates are included in IF-77 [20, p. 103]; i.e., (1) equatorial, (2) continental sub-tropical, (3) maritime sub-tropical, (4) desert, (5) mediterranean, (6) continental temperate, (7a) maritime temperate overland, (7b) maritime temperate oversea, and (8) polar. The formulation used is based on algebraic expressions fitted to modified versions of curves provided in CCIR Report 238-4 [7] by Hufford and Longley [DOC-BL, informal communication; 15, Sec. 4.3; 29, Sec. 4.4.2.5] and may be summarized as follows:

$$A_{Y} = \left\{ \begin{array}{l} 0 \text{ if } A_{Y1} \leq 0 \\ 10 \text{ if } A_{Y1} \geq 10 \\ A_{Y1} \text{ otherwise} \end{array} \right\} \quad (243)$$

$$Y_{e}(q<0.1) = \left| \begin{array}{l} \text{lesser of } [Y_{e1}(q) \text{ or } Y_{T}] \text{ for lobing} \\ \\ \text{lesser of } [Y_{e1}(q) \text{ or} \\ L_{br} + A_{Y} - (L_{bf} - c_{Y})] \\ \text{otherwise} \end{array} \right\} \text{ dB} \quad (244)$$

where c_Y is 6, 5.8, and 5 dB for q values of 0.0001, 0.001, and 0.01, respectively,

$$Y_{e}(q>0.1) \equiv Y_{e1}(q) \text{ dB} . \quad (245)$$

10.1.1 Time Blocks

Long-term variability options for IF-77 include variabilities appropriate for the time blocks shown in Table 1 [20, p. 103]. These blocks and seasonal groupings are used to describe the diurnal and seasonal variations in a continental temperate climate [34, Sec. III.7.1]. They are incorporated into (235) by selecting appropriate constants from Rice et al. [34, Tables III.2, III.3, and III.4]. The expressions for $g(0.1,f)$ and $g(0.9,f)$ given in (233) are used for time block variabilities.

If a combination of time blocks is appropriate, various distributions can be mixed (Sec. 10.6).

10.1.2 Climates

Options to use various climates are included in IF-77 [20, p. 103]; i.e., (1) equatorial, (2) continental sub-tropical, (3) maritime sub-tropical, (4) desert, (5) mediterranean, (6) continental temperate, (7a) maritime temperate overland, (7b) maritime temperate oversea, and (8) polar. The formulation used is based on algebraic expressions fitted to modified versions of curves provided in CCIR Report 238-4 [7] by Hufford and Longley [DOC-BL, informal communication; 15, Sec. 4.3; 29, Sec. 4.4.2.5] and may be summarized as follows:

$$A_{Y} = \left\{ \begin{array}{l} 0 \text{ if } A_{Y1} \leq 0 \\ 10 \text{ if } A_{Y1} \geq 10 \\ A_{Y1} \text{ otherwise} \end{array} \right\} \quad (243)$$

$$Y_{e}(q<0.1) = \left| \begin{array}{l} \text{lesser of } [Y_{e1}(q) \text{ or } Y_{T}] \text{ for lobing} \\ \\ \text{lesser of } [Y_{e1}(q) \text{ or} \\ L_{br} + A_{Y} - (L_{bf} - c_{Y})] \\ \text{otherwise} \end{array} \right\} \text{ dB} \quad (244)$$

where c_Y is 6, 5.8, and 5 dB for q values of 0.0001, 0.001, and 0.01, respectively,

$$Y_{e}(q>0.1) \equiv Y_{e1}(q) \text{ dB} . \quad (245)$$

10.1.1 Time Blocks

Long-term variability options for IF-77 include variabilities appropriate for the time blocks shown in Table 1 [20, p. 103]. These blocks and seasonal groupings are used to describe the diurnal and seasonal variations in a continental temperate climate [34, Sec. III.7.1]. They are incorporated into (235) by selecting appropriate constants from Rice et al. [34, Tables III.2, III.3, and III.4]. The expressions for $g(0.1,f)$ and $g(0.9,f)$ given in (233) are used for time block variabilities.

If a combination of time blocks is appropriate, various distributions can be mixed (Sec. 10.6).

10.1.2 Climates

Options to use various climates are included in IF-77 [20, p. 103]; i.e., (1) equatorial, (2) continental sub-tropical, (3) maritime sub-tropical, (4) desert, (5) mediterranean, (6) continental temperate, (7a) maritime temperate overland, (7b) maritime temperate oversea, and (8) polar. The formulation used is based on algebraic expressions fitted to modified versions of curves provided in CCIR Report 238-4 [7] by Hufford and Longley [DOC-BL, informal communication; 15, Sec. 4.3; 29, Sec. 4.4.2.5] and may be summarized as follows:

$$F_{\Delta r} = \left[\begin{cases} 1 & \text{for } \Delta r_g > 10\lambda \\ 0 & \text{otherwise} \end{cases} \right] \left[\begin{cases} \text{for lobing} \\ \text{option [20, p. 99]} \end{cases} \right] \left[\begin{cases} 1 & \text{for } \Delta r_g \geq \lambda/2 \\ 0.1 & \text{for } \Delta r_g \leq \lambda/6 \\ \dfrac{1.1 - 0.9 \cos[3\pi(\Delta r_g - \lambda/6)/\lambda]}{2} & \text{otherwise} \end{cases} \right] \quad (249)$$

where Δr_g is from (114b) and λ is from (10b)

$$R_s = R_{Tg} \left(F_{AY} F_{\Delta r} \right) \quad (250)$$

where R_s^2 is the relative contribution of specular reflection to surface reflection multipath power, and R_{Tg} is from (119a), R_d from (129) may be expressed as:

$$R_d = R_{Tg} \left(\frac{F_{d\sigma h}}{F_{\sigma h} D_v} \right) \quad (251)$$

where R_d^2 is the relative contribution of diffuse reflection to surface reflection multipath power, $F_{d\sigma h}$ is from (128), $F_{\sigma h}$ is from (127), and D_v is from (122),

$$W_R = \left\{ \begin{cases} \left(R_s^2 + R_d^2 \right) / g_D^2 & \text{for LOS } (d \leq d_{ML}) \\ 0 & \text{otherwise} \end{cases} \right\} \quad (252)$$

where d is the path length obtained from (118) for LOS paths, d_{ML} is from (43), and g_D is from (141).

10.3 Tropospheric Multipath

Tropospheric multipath is caused by reflections from atmospheric sheets or elevated layers, or additional direct (nonreflected) wave paths [2; 9, Sec. 3.1], and may be present when antenna directivity is sufficient to make surface reflections negligible. It is considered as part of the short-term (within the hour) variabil-

$$F_{\Delta r} = \left[\begin{cases} 1 & \text{for } \Delta r_g > 10\lambda \\ 0 & \text{otherwise} \end{cases} \right] \left[\begin{cases} \text{for lobing} \\ \text{option [20, p. 99]} \end{cases} \right] \left[\begin{cases} 1 & \text{for } \Delta r_g \geq \lambda/2 \\ 0.1 & \text{for } \Delta r_g \leq \lambda/6 \\ \dfrac{1.1 - 0.9 \cos[3\pi(\Delta r_g - \lambda/6)/\lambda]}{2} & \text{otherwise} \end{cases} \right] \quad (249)$$

where Δr_g is from (114b) and λ is from (10b)

$$R_s = R_{Tg} \left(F_{AY} F_{\Delta r} \right) \quad (250)$$

where R_s^2 is the relative contribution of specular reflection to surface reflection multipath power, and R_{Tg} is from (119a), R_d from (129) may be expressed as:

$$R_d = R_{Tg} \left(\frac{F_{d\sigma h}}{F_{\sigma h} D_v} \right) \quad (251)$$

where R_d^2 is the relative contribution of diffuse reflection to surface reflection multipath power, $F_{d\sigma h}$ is from (128), $F_{\sigma h}$ is from (127), and D_v is from (122),

$$W_R = \left\{ \begin{cases} \left(R_s^2 + R_d^2 \right) / g_D^2 & \text{for LOS } (d \leq d_{ML}) \\ 0 & \text{otherwise} \end{cases} \right\} \quad (252)$$

where d is the path length obtained from (118) for LOS paths, d_{ML} is from (43), and g_D is from (141).

10.3 Tropospheric Multipath

Tropospheric multipath is caused by reflections from atmospheric sheets or elevated layers, or additional direct (nonreflected) wave paths [2; 9, Sec. 3.1], and may be present when antenna directivity is sufficient to make surface reflections negligible. It is considered as part of the short-term (within the hour) variabil-

Relative powers W_a and W_R from (252) are combined to determine K, which is the ratio in decibels between the steady component (e.g., direct ray), and the Rayleigh fading component (e.g., surface reflection and tropospheric multipath) using:

$$K = -10 \log (W_R + W_a) \quad \text{dB} \tag{258}$$

The Nakagami-Rice probability distribution for $Y_T(q)$ of (229) is then selected from the Rice et al. curves [34, p. V-8] by using K.

10.4 Rain Attenuation

The rain attenuation model used in IF-77 is largely based on material in informal papers by C. A. Samson (DOC-BL) on "Radio Propagation Through Precipitation" and "Rain Rate Distribution Curves." This discussion is a shortened version of the description previously provided [15, Sec. 4.4], and the maps and tables provided there are not repeated here.

Two options for rain attenuation are available in IF-77. The first is for use in a "worst case" type analysis where a particular rainfall attenuation rate is assumed for the in-storm path length, and the additional path attenuation associated with rain is simply taken as the product of this attenuation rate (in dB/km) and the in-storm ray length [20, p. 94]. This ray length is determined in accordance with the method discussed in step 4 of option two.

Option two involves computer input of rain zone (which determines a rainfall rate distribution) and storm size [20, p. 94]. Storm size (diameter or long dimension) is assumed to be one of three options: 5, 10, or 20 km (corresponding approximately to a relatively small, average, or very large thunderstorm). The maximum distance used in calculating path attenuation with this option is the storm size since it is assumed that only one storm is on the path at a time. The process used to include rain attenuation estimates in IF-77 for this option may be summarized as follows:

1. Determine point rain rates. Point rain rates (rate at a particular point of observation) not exceeded for specific fractions of the time are determined for the rain zone of interest [15, p. 38].

2. Determine path average rain rates. Each point rain rate resulting from step 1 is converted to a path average rain rate by using linear interpolation to obtain a multiplying factor [15, p. 39].

Relative powers W_a and W_R from (252) are combined to determine K, which is the ratio in decibels between the steady component (e.g., direct ray), and the Rayleigh fading component (e.g., surface reflection and tropospheric multipath) using:

$$K = -10 \log (W_R + W_a) \quad \text{dB} \tag{258}$$

The Nakagami-Rice probability distribution for $Y_T(q)$ of (229) is then selected from the Rice et al. curves [34, p. V-8] by using K.

10.4 Rain Attenuation

The rain attenuation model used in IF-77 is largely based on material in informal papers by C. A. Samson (DOC-BL) on "Radio Propagation Through Precipitation" and "Rain Rate Distribution Curves." This discussion is a shortened version of the description previously provided [15, Sec. 4.4], and the maps and tables provided there are not repeated here.

Two options for rain attenuation are available in IF-77. The first is for use in a "worst case" type analysis where a particular rainfall attenuation rate is assumed for the in-storm path length, and the additional path attenuation associated with rain is simply taken as the product of this attenuation rate (in dB/km) and the in-storm ray length [20, p. 94]. This ray length is determined in accordance with the method discussed in step 4 of option two.

Option two involves computer input of rain zone (which determines a rainfall rate distribution) and storm size [20, p. 94]. Storm size (diameter or long dimension) is assumed to be one of three options: 5, 10, or 20 km (corresponding approximately to a relatively small, average, or very large thunderstorm). The maximum distance used in calculating path attenuation with this option is the storm size since it is assumed that only one storm is on the path at a time. The process used to include rain attenuation estimates in IF-77 for this option may be summarized as follows:

1. Determine point rain rates. Point rain rates (rate at a particular point of observation) not exceeded for specific fractions of the time are determined for the rain zone of interest [15, p. 38].

2. Determine path average rain rates. Each point rain rate resulting from step 1 is converted to a path average rain rate by using linear interpolation to obtain a multiplying factor [15, p. 39].

10.5 Ionospheric Scintillation

Variability associated with ionospheric scintillation, $Y_I(q)$ for (229), for paths that pass through the ionosphere (i.e., on earth/satellite paths) at an altitude of about 350 km is included in IF-77. This variability may be specified directly by the selection of a scintillation index group or by using a weighted mixture of distributions where the weighting factors are estimated for specific problems [20, p. 91; 15, Sec. 4.5]. Provisions are included to allow $Y_I(q)$ to change with earth facility latitude when a geostationary satellite is involved and the earth facility locations are along the subsatellite meridian. When this provision is used, $Y_{136}(q)$ is obtained from previously prepared 136 MHz data [15, p. 45] and $Y_I(q)$ is calculated as follows:

$$m = \begin{cases} 1 & \text{for } \theta_{FL} \leq 17^\circ \text{ or } \theta_{FL} \geq 52^\circ \\ 1 + (\theta_{FL} - 17)/7 & \text{for } 17^\circ < \theta_{FL} < 24^\circ \\ & \\ 2 & \text{for } 24^\circ < \theta_{FL} \leq 45^\circ \\ 1 + (52 - \theta_{FL})/7 & \text{for } 45^\circ \leq \theta_{FL} \leq 52^\circ \end{cases} \qquad (262)$$

where θ_{FL} is the magnitude of the earth facilities latitude in degrees, and

$$Y_I(q) = (136/f)^m Y_{136}(q) \quad \text{dB} \qquad (263)$$

Even though this scaling factor is built into the programs that utilize IF-77, only minor program modifications would be required to use other simple scaling methods. In addition, the distribution mixing methods of Section 10.6 could be used to create $Y_I(q)$'s applicable to specific situations.

10.6 Mixing Distributions

Subroutines have been incorporated into the IF-77 computer programs to allow the distributions that characterize portions of the variability associated with a particular model component to be mixed in order to obtain the total variability for that component. For example, different fractions of the time may be characterized

10.5 Ionospheric Scintillation

Variability associated with ionospheric scintillation, $Y_I(q)$ for (229), for paths that pass through the ionosphere (i.e., on earth/satellite paths) at an altitude of about 350 km is included in IF-77. This variability may be specified directly by the selection of a scintillation index group or by using a weighted mixture of distributions where the weighting factors are estimated for specific problems [20, p. 91; 15, Sec. 4.5]. Provisions are included to allow $Y_I(q)$ to change with earth facility latitude when a geostationary satellite is involved and the earth facility locations are along the subsatellite meridian. When this provision is used, $Y_{136}(q)$ is obtained from previously prepared 136 MHz data [15, p. 45] and $Y_I(q)$ is calculated as follows:

$$m = \begin{cases} 1 & \text{for } \theta_{FL} \leq 17^\circ \text{ or } \theta_{FL} \geq 52^\circ \\ 1 + (\theta_{FL} - 17)/7 & \text{for } 17^\circ < \theta_{FL} < 24^\circ \\ & \\ 2 & \text{for } 24^\circ < \theta_{FL} \leq 45^\circ \\ 1 + (52 - \theta_{FL})/7 & \text{for } 45^\circ \leq \theta_{FL} \leq 52^\circ \end{cases} \qquad (262)$$

where θ_{FL} is the magnitude of the earth facilities latitude in degrees, and

$$Y_I(q) = (136/f)^m Y_{136}(q) \quad \text{dB} \qquad (263)$$

Even though this scaling factor is built into the programs that utilize IF-77, only minor program modifications would be required to use other simple scaling methods. In addition, the distribution mixing methods of Section 10.6 could be used to create $Y_I(q)$'s applicable to specific situations.

10.6 Mixing Distributions

Subroutines have been incorporated into the IF-77 computer programs to allow the distributions that characterize portions of the variability associated with a particular model component to be mixed in order to obtain the total variability for that component. For example, different fractions of the time may be characterized

When this process is used to mix distributions of long-term variability, the required variability functions are obtained from:

$$V_c(q) = [V(0.5) + Y(q)]_c \quad \text{dB} \tag{265}$$

where $[\ldots]_c$ indicates that the $V(0.5)$ and $Y(q)$ are appropriate for the conditions (e.g., time block or climate) associated with a particular value of the subscript c. For example, $V(0.5)$ and $Y(q)$ values for different climates can be obtained by using (247) with (236, 237) and mixing can be used to estimate variability for areas near a border between two different climate types. After mixing, $Y(q)$ values needed for (239) may be obtained by using:

$$Y(q) = V(q) - V(0.5) \quad \text{dB} \tag{266}$$

where all variables in (266) are associated with the resulting mixed distribution. Similarly, when mixing variabilities associated with ionospheric scintillation,

$$Y_I(q_i) = [Y_I^*(q_i)]_c \quad \text{dB} \tag{267}$$

and the distribution resulting from the mixing is taken as $Y_I^*(q_i)$ for later calculations.

11. SUMMARY

The ITS-77 electromagnetic wave propagation model was discussed, and references were provided so that more information on specific items could be obtained. A brief description of the model provided in Section 2 is followed by a systematic discussion of model components. Readers with a further interest in ITS-77 are encouraged to obtain a copy of the "Applications Guide for Propagation and Interference Analysis Computer Programs (0.1 to 20 GHz)" [20].

When this process is used to mix distributions of long-term variability, the required variability functions are obtained from:

$$V_c(q) = [V(0.5) + Y(q)]_c \quad \text{dB} \tag{265}$$

where $[\ldots]_c$ indicates that the $V(0.5)$ and $Y(q)$ are appropriate for the conditions (e.g., time block or climate) associated with a particular value of the subscript c. For example, $V(0.5)$ and $Y(q)$ values for different climates can be obtained by using (247) with (236, 237) and mixing can be used to estimate variability for areas near a border between two different climate types. After mixing, $Y(q)$ values needed for (239) may be obtained by using:

$$Y(q) = V(q) - V(0.5) \quad \text{dB} \tag{266}$$

where all variables in (266) are associated with the resulting mixed distribution. Similarly, when mixing variabilities associated with ionospheric scintillation,

$$Y_I(q_i) = [Y_I^*(q_i)]_c \quad \text{dB} \tag{267}$$

and the distribution resulting from the mixing is taken as $Y_I^*(q_i)$ for later calculations.

11. SUMMARY

The ITS-77 electromagnetic wave propagation model was discussed, and references were provided so that more information on specific items could be obtained. A brief description of the model provided in Section 2 is followed by a systematic discussion of model components. Readers with a further interest in ITS-77 are encouraged to obtain a copy of the "Applications Guide for Propagation and Interference Analysis Computer Programs (0.1 to 20 GHz)" [20].

A_F	Attenuation line intercept [dB] of rounded earth diffraction for path F-O-ML (Figure 7), from (54,78).
A_I	Effective area [dB-sq m] of an isotropic antenna, from (9).
A_{KA}	Knife-edge diffraction attenuation [dB] for path F-O-A (Figure 7), from (93).
A_{KML}	Knife-edge diffraction attenuation [dB] for path F-O-ML (Figure 7), from (87).
A_{K5}	Knife-edge diffraction attenuation [dB] at d_5, from (168).
A_{LOS}	Line-of-sight attenuation [dB], from (177).
A_m	A parameter [km] used in tropospheric scatter calculations, from (183).
A_{ML}	Combined diffraction attenuation [dB] at d_{ML}, from (95).
A_o	A_{RO} [dB] at d_0, from (175).
A_0	Attenuation line intercept [dB] of rounded earth diffraction path O-A (Figure 7), from (54,78).
A_p	Rounded earth diffraction attenuation [dB] for path p, from (54,78).
A_{rA}	A_{rF} [dB] at d_A, from (85).
A_{rF}	Rounded earth diffraction attenuation [dB] for path F-O-A (Figure 7), from (85).
A_{rML}	A_{rF} [dB] at d_{ML}, from (85).
A_{r0}	Rounded earth diffraction attenuation [dB] for path O-A (Figure 7) at distance d_{LSA}, from (86).
A_{RO}	Attenuation [dB] in the line-of-sight region where the diffraction effects associated with terrain are negligible ($d < d_0$), from (175).
$A_r(q)$	Attenuation [dB] due to rain for a fraction of time q, from (260).
$A_{rr}(q)$	Attenuation rate [dB/km] associated with rain and a fraction of time q, (Sec. 10.4, Step 3).
A_{r5}	A_{rF} [dB] at d_5, from (169).
A_s	Forward scatter attenuation [dB], from (220).

A_F	Attenuation line intercept [dB] of rounded earth diffraction for path F-O-ML (Figure 7), from (54,78).
A_I	Effective area [dB-sq m] of an isotropic antenna, from (9).
A_{KA}	Knife-edge diffraction attenuation [dB] for path F-O-A (Figure 7), from (93).
A_{KML}	Knife-edge diffraction attenuation [dB] for path F-O-ML (Figure 7), from (87).
A_{K5}	Knife-edge diffraction attenuation [dB] at d_5, from (168).
A_{LOS}	Line-of-sight attenuation [dB], from (177).
A_m	A parameter [km] used in tropospheric scatter calculations, from (183).
A_{ML}	Combined diffraction attenuation [dB] at d_{ML}, from (95).
A_o	A_{RO} [dB] at d_0, from (175).
A_0	Attenuation line intercept [dB] of rounded earth diffraction path O-A (Figure 7), from (54,78).
A_p	Rounded earth diffraction attenuation [dB] for path p, from (54,78).
A_{rA}	A_{rF} [dB] at d_A, from (85).
A_{rF}	Rounded earth diffraction attenuation [dB] for path F-O-A (Figure 7), from (85).
A_{rML}	A_{rF} [dB] at d_{ML}, from (85).
A_{r0}	Rounded earth diffraction attenuation [dB] for path O-A (Figure 7) at distance d_{LSA}, from (86).
A_{RO}	Attenuation [dB] in the line-of-sight region where the diffraction effects associated with terrain are negligible ($d < d_0$), from (175).
$A_r(q)$	Attenuation [dB] due to rain for a fraction of time q, from (260).
$A_{rr}(q)$	Attenuation rate [dB/km] associated with rain and a fraction of time q, (Sec. 10.4, Step 3).
A_{r5}	A_{rF} [dB] at d_5, from (169).
A_s	Forward scatter attenuation [dB], from (220).

dB/km	Attenuation [dB] per unit length [km].
dB-sq m	Units for effective area in terms of decibels greater than an effective area of 1 square meter; i.e., 10 log (area in square meters).
dBW	Power in decibels greater than 1 watt.
dB-W/sq m	Units of power density in terms of decibels greater than 1 watt per square meter; i.e., 10 log (power density expressed in watts per square meter).
dN	A parameter [per km] used in tropospheric scatter calculations, from (184).
d_{dA}	A facility-to-aircraft (Figure 7) distance [km], from (96).
d_{dc}	Counterpoise diameter [km], a model input parameter [20, p. 88, FACILITY ANTENNA COUNTERPOISE DIAMETER].
d_{dd}	Initial estimate of d_0, from (171).
d_{de}	Effective distance [km], from (232).
d_{dh}	A distance [km] used in facility horizon determination, from (35).
d_{dLE1}	An initial value for the facility horizon distance [km] that is based on effective earth radius geometry, and shown in Figure 4. It may be specified [20, p. 90] or calculated as indicated in Figure 5, from (33,36).
d_{LM}	Maximum distance [km] for which the facility-to-aircraft path has a common horizon, from (45).
$d_{LO1,2}$	Smooth earth horizon distances [km] for path O-A (Figure 7), from (52,53).
d_{Lp}	Total horizon distances [km] for path p, from (59).
$d_{Lp1,2}$	Radio horizon distances [km] for path p, from (52,53).
d_{Lq}	Smooth earth horizon distances [km] determined via ray tracing (Sec. 3) over a 9000-km (4860 n mi) earth, discussed after (231).
d_{dLR2}	Horizon distance for aircraft shown in Figure 4 and discussed preceding (43).

dB/km	Attenuation [dB] per unit length [km].
dB-sq m	Units for effective area in terms of decibels greater than an effective area of 1 square meter; i.e., 10 log (area in square meters).
dBW	Power in decibels greater than 1 watt.
dB-W/sq m	Units of power density in terms of decibels greater than 1 watt per square meter; i.e., 10 log (power density expressed in watts per square meter).
dN	A parameter [per km] used in tropospheric scatter calculations, from (184).
d_{dA}	A facility-to-aircraft (Figure 7) distance [km], from (96).
d_{dc}	Counterpoise diameter [km], a model input parameter [20, p. 88, FACILITY ANTENNA COUNTERPOISE DIAMETER].
d_{dd}	Initial estimate of d_0, from (171).
d_{de}	Effective distance [km], from (232).
d_{dh}	A distance [km] used in facility horizon determination, from (35).
d_{dLE1}	An initial value for the facility horizon distance [km] that is based on effective earth radius geometry, and shown in Figure 4. It may be specified [20, p. 90] or calculated as indicated in Figure 5, from (33,36).
d_{LM}	Maximum distance [km] for which the facility-to-aircraft path has a common horizon, from (45).
$d_{LO1,2}$	Smooth earth horizon distances [km] for path O-A (Figure 7), from (52,53).
d_{Lp}	Total horizon distances [km] for path p, from (59).
$d_{Lp1,2}$	Radio horizon distances [km] for path p, from (52,53).
d_{Lq}	Smooth earth horizon distances [km] determined via ray tracing (Sec. 3) over a 9000-km (4860 n mi) earth, discussed after (231).
d_{dLR2}	Horizon distance for aircraft shown in Figure 4 and discussed preceding (43).

$d_{3,4}$ Distances [km] used in rounded earth diffraction calculation, from (60,61).

d_5 A distance [km] calculated from (162).

$d_{\lambda/6}$ The largest distance [km] at which a free-space value of basic transmission loss is obtained in two-ray model of reflection from a smooth earth with an effective reflection coefficient of -1. This occurs when the path length difference, Δr from (114), is equal to $\lambda/6$.

DOC-BL United States Department of Commerce, Boulder Laboratories.

DOT United States Department of Transportation.

$D/U(q)$ Desired-to-undesired signal ratio [dB] exceeded for at least a fraction q of the time. These values may represent instantaneous levels or hourly median levels depending upon the time availability option selected [20, p. 103] and are calculated via (11).

D_{bv} Divergence factor, from (122).

$D_{1,2}$ Distances [km] shown in Figure 8 and calculated via (109).

e 2.718281828.

eq. Equation.

exp( ) Exponential; e.g., $\exp(2) = e^2$ or $R\exp(-j\phi) = Re^{-\sqrt{-1}\phi}$ is a phasor with magnitude R and a lag of ϕ radians.

EIRP Equivalent isotropically radiated power [dBW] as defined by (7).

EIRPG EIRP [dBW] increased by the main beam gain [dBi] of the receiving antenna as in (6).

f Frequency [MHZ], an input parameter [20, p. 82].

fss Facility site Surface (Figure 2).

$f_{c1,2}$ A parameter used in $G_{\bar{h}}^{X}$ weighting factor and calculated from (81).

$f_{g,cw2,5}$ Knife-edge diffraction loss factors determined using Fresnel integrals, from (137, 92, 167).

$f_{m1,2,3}$ Parameters used in the normally used variability formulation and discussed following (235).

$f_{\theta h}$ Elevation angle correction factor, from (238).

$d_{3,4}$ Distances [km] used in rounded earth diffraction calculation, from (60,61).

d_5 A distance [km] calculated from (162).

$d_{\lambda/6}$ The largest distance [km] at which a free-space value of basic transmission loss is obtained in two-ray model of reflection from a smooth earth with an effective reflection coefficient of -1. This occurs when the path length difference, Δr from (114), is equal to $\lambda/6$.

DOC-BL United States Department of Commerce, Boulder Laboratories.

DOT United States Department of Transportation.

$D/U(q)$ Desired-to-undesired signal ratio [dB] exceeded for at least a fraction q of the time. These values may represent instantaneous levels or hourly median levels depending upon the time availability option selected [20, p. 103] and are calculated via (11).

D_{bv} Divergence factor, from (122).

$D_{1,2}$ Distances [km] shown in Figure 8 and calculated via (109).

e 2.718281828.

eq. Equation.

exp( ) Exponential; e.g., $\exp(2) = e^2$ or $R\exp(-j\phi) = Re^{-\sqrt{-1}\phi}$ is a phasor with magnitude R and a lag of ϕ radians.

EIRP Equivalent isotropically radiated power [dBW] as defined by (7).

EIRPG EIRP [dBW] increased by the main beam gain [dBi] of the receiving antenna as in (6).

f Frequency [MHZ], an input parameter [20, p. 82].

fss Facility site Surface (Figure 2).

$f_{c1,2}$ A parameter used in $G_{\bar{h}}^{X}$ weighting factor and calculated from (81).

$f_{g,cw2,5}$ Knife-edge diffraction loss factors determined using Fresnel integrals, from (137, 92, 167).

$f_{m1,2,3}$ Parameters used in the normally used variability formulation and discussed following (235).

$f_{\theta h}$ Elevation angle correction factor, from (238).

$g_{vD1,2}$	Voltage gain [V/V] similar to $g_{D1,2}$, but specifically for vertical polarization.
$g_{vR1,2}$	Voltage gain [V/V] similar to $g_{R1,2}$, but specifically for vertical polarization.
GHz	Gigahertz (10^9 Hz).
$G_{ET,R}$	Gain [dBi] of the transmitting or receiving antenna at an appropriate elevation angle, from (4).
$G_{\overline{hl},2}$	Values [dB] for the residual height gain function, from (83).
$G_{\overline{hF1,2}}$	$G_{\overline{hp1,2}}$ [dB] for path F-O-ML (Figure 7), from (56,84).
$G_{\overline{hO1,2}}$	$G_{\overline{hp1,2}}$ [dB] for path O-A (Figure 7), from (56,84).
$G_{\overline{hp1,2}}$	Values [dB] for the weighted residual height gain function (Sec. 4.2) for path p, from (56,84).
$G_{NT,R}$	Normalized gain of the transmitting or receiving antenna at appropriate elevation angle in decibels greater than the main beam (G_T or G_R), from (145).
$G_{R1,2}$	Gains [dB] $g_{R1,2}$ expressed in decibels, from (139).
$G_{T,R}$	Gain [dBi] of the transmitting or receiving main beam for (4,6,7).
$G_{W1,2}$	Weighting factor, from (82).
$G_{1,2,3,4}$	Parameters [dB] calculated from (71).
h	Ray height [km] above msl used in (17).
h_c	Height [km] of facility counterpoise above ground at the facility site, an input parameter [20, p. 88].
h_e	An effective height [km], from (34).
h_{em2}	Effective aircraft altitude [km] above msl, from (160).
$h_{ep1,2}$	Effective antenna heights [km] for path p, from (50,51).
$h_{e1,2}$	Effective antenna height [km] above h_r (Figure 3), from (24), and shown in Figure 3.

$g_{vD1,2}$	Voltage gain [V/V] similar to $g_{D1,2}$, but specifically for vertical polarization.
$g_{vR1,2}$	Voltage gain [V/V] similar to $g_{R1,2}$, but specifically for vertical polarization.
GHz	Gigahertz (10^9 Hz).
$G_{ET,R}$	Gain [dBi] of the transmitting or receiving antenna at an appropriate elevation angle, from (4).
$G_{\overline{hl},2}$	Values [dB] for the residual height gain function, from (83).
$G_{\overline{hF1,2}}$	$G_{\overline{hp1,2}}$ [dB] for path F-O-ML (Figure 7), from (56,84).
$G_{\overline{hO1,2}}$	$G_{\overline{hp1,2}}$ [dB] for path O-A (Figure 7), from (56,84).
$G_{\overline{hp1,2}}$	Values [dB] for the weighted residual height gain function (Sec. 4.2) for path p, from (56,84).
$G_{NT,R}$	Normalized gain of the transmitting or receiving antenna at appropriate elevation angle in decibels greater than the main beam (G_T or G_R), from (145).
$G_{R1,2}$	Gains [dB] $g_{R1,2}$ expressed in decibels, from (139).
$G_{T,R}$	Gain [dBi] of the transmitting or receiving main beam for (4,6,7).
$G_{W1,2}$	Weighting factor, from (82).
$G_{1,2,3,4}$	Parameters [dB] calculated from (71).
h	Ray height [km] above msl used in (17).
h_c	Height [km] of facility counterpoise above ground at the facility site, an input parameter [20, p. 88].
h_e	An effective height [km], from (34).
h_{em2}	Effective aircraft altitude [km] above msl, from (160).
$h_{ep1,2}$	Effective antenna heights [km] for path p, from (50,51).
$h_{e1,2}$	Effective antenna height [km] above h_r (Figure 3), from (24), and shown in Figure 3.

IF-73	ITS-FAA-1973 propagation model.
IF-77	ITS-FAA-1977 propagation model.
ITS	Institute for Telecommunication Sciences.
j	$\sqrt{-1}$ as in (154) or index (1 to N) for specific transmission loss distributions used in the distribution mixing process (Sec. 10.6).
k_{ka}	An adjusted earth radius factor, from (103).
K	The ratio [dB] between the steady component of received power and the Rayleigh fading component that is used to determine the appropriate Nagagami-Rice distribution [34, p. V-81] for $Y_T(q)$, from (258).
$K_{d1,2,3,4}$	Rounded earth diffraction parameters, from (65).
$K_{F1,2}$	Rounded earth diffraction parameters, from (67).
K_{LOS}	K_t values in the line-of-sight region, from (254).
K_{ML}	K values at the radio horizon; i.e., K_{LOS} at d = d_{ML}, from (254).
K_{Kt}	K value associated with tropospheric multipath, from (256).
$K_{K1,2,3,4}$	Rounded earth diffraction parameters, from (66).
ℓ	Total ray length [km] in scatter calculation, from (204).
$\log_{10}$	Common (base 10) logarithm.
$\log_e$	Natural (base e) logarithm.
$\ell_{1,2}$	Ray lengths [km] to the cross-over point of the common volume in tropospheric scatter calculations, from (203).
LOS	Line-of-sight.
$L(q)$	Transmission loss [dB] values not exceeded during a fraction q of the time. These values may represent instantaneous levels depending upon the time availability option selected (Sec. 10), and are calculated using (1).
L_{bf}	Basic transmission loss [dB] for the free space, from (226).

IF-73	ITS-FAA-1973 propagation model.
IF-77	ITS-FAA-1977 propagation model.
ITS	Institute for Telecommunication Sciences.
j	$\sqrt{-1}$ as in (154) or index (1 to N) for specific transmission loss distributions used in the distribution mixing process (Sec. 10.6).
k_{ka}	An adjusted earth radius factor, from (103).
K	The ratio [dB] between the steady component of received power and the Rayleigh fading component that is used to determine the appropriate Nagagami-Rice distribution [34, p. V-81] for $Y_T(q)$, from (258).
$K_{d1,2,3,4}$	Rounded earth diffraction parameters, from (65).
$K_{F1,2}$	Rounded earth diffraction parameters, from (67).
K_{LOS}	K_t values in the line-of-sight region, from (254).
K_{ML}	K values at the radio horizon; i.e., K_{LOS} at d = d_{ML}, from (254).
K_{Kt}	K value associated with tropospheric multipath, from (256).
$K_{K1,2,3,4}$	Rounded earth diffraction parameters, from (66).
ℓ	Total ray length [km] in scatter calculation, from (204).
$\log_{10}$	Common (base 10) logarithm.
$\log_e$	Natural (base e) logarithm.
$\ell_{1,2}$	Ray lengths [km] to the cross-over point of the common volume in tropospheric scatter calculations, from (203).
LOS	Line-of-sight.
$L(q)$	Transmission loss [dB] values not exceeded during a fraction q of the time. These values may represent instantaneous levels depending upon the time availability option selected (Sec. 10), and are calculated using (1).
L_{bf}	Basic transmission loss [dB] for the free space, from (226).

NTIA	National Telecommunications and Information Administration.
N_o	Minimum monthly mean surface refractivity (N-units) referred to msl, an input parameter [20, p. 94].
N_s	Minimum monthly mean surface refractive (N-units) at effective reflection surface, calculated from N_o via (14).
$P_a(q)$	Power [dBW] that is available at the terminal of an ideal (loss-less) receiving antenna for at least a fraction q of the time, from (5).
P_{TR}	Total power [dBW] radiated from the transmitting antenna, used in (7).
q	Dimensionless fraction of time used in time availability specification; e.g., in $L_b(0.1)$, q = 0.1 implies a time availability of 10 percent.
$q_{l1,2}$	Parameters used in tropospheric scatter calculations, from (216).
$q_{l1,i,M}$	Time availabilities for mixed distributions that correspond to specific transmission loss levels, from (264).
$q_{l1,ij,MN}$	Time availabilities for each transmission loss level (index i) of each transmission loss distribution (index j) involved in the distribution mixing distribution (Sec. 10.6).
$Q_{al,2}$	Parameters used in tropospheric scatter calculations, from (189).
$Q_{Al,2}$	Parameters used in tropospheric scatter calculations, from (193).
$Q_{bl,2}$	Parameters used in tropospheric scatter calculations, from (190).
$Q_{Bl,2}$	Parameters used in tropospheric scatter calculations, from (194).
$Q_{ol,2}$	Parameters used in tropospheric scatter calculations, from (188).
r	Ray length [km] used in the calculation of free space loss, from (225).
r_{BH}	Ray length [km] for beyond-the-horizon paths, from (224).
r_c	A distance [km], from (131).
$r_{eo,s,w}$	Effective ray lengths [km] for attenuation associated with oxygen absorption, (r_{eo}), rain storm attenuation (r_{es}), and water vapor absorption (r_{ew}), from (227).

NTIA	National Telecommunications and Information Administration.
N_o	Minimum monthly mean surface refractivity (N-units) referred to msl, an input parameter [20, p. 94].
N_s	Minimum monthly mean surface refractive (N-units) at effective reflection surface, calculated from N_o via (14).
$P_a(q)$	Power [dBW] that is available at the terminal of an ideal (loss-less) receiving antenna for at least a fraction q of the time, from (5).
P_{TR}	Total power [dBW] radiated from the transmitting antenna, used in (7).
q	Dimensionless fraction of time used in time availability specification; e.g., in $L_b(0.1)$, q = 0.1 implies a time availability of 10 percent.
$q_{l1,2}$	Parameters used in tropospheric scatter calculations, from (216).
$q_{l1,i,M}$	Time availabilities for mixed distributions that correspond to specific transmission loss levels, from (264).
$q_{l1,ij,MN}$	Time availabilities for each transmission loss level (index i) of each transmission loss distribution (index j) involved in the distribution mixing distribution (Sec. 10.6).
$Q_{al,2}$	Parameters used in tropospheric scatter calculations, from (189).
$Q_{Al,2}$	Parameters used in tropospheric scatter calculations, from (193).
$Q_{bl,2}$	Parameters used in tropospheric scatter calculations, from (190).
$Q_{Bl,2}$	Parameters used in tropospheric scatter calculations, from (194).
$Q_{ol,2}$	Parameters used in tropospheric scatter calculations, from (188).
r	Ray length [km] used in the calculation of free space loss, from (225).
r_{BH}	Ray length [km] for beyond-the-horizon paths, from (224).
r_c	A distance [km], from (131).
$r_{eo,s,w}$	Effective ray lengths [km] for attenuation associated with oxygen absorption, (r_{eo}), rain storm attenuation (r_{es}), and water vapor absorption (r_{ew}), from (227).

SHF	Super High Frequency [3 to 30 GHz].
Sin-'	Inverse sine with principal value.
S_e	Scattering efficiency term [dB] used in tropospheric scatter calculations, from (208).
$S_{R(q)}$	Power density at receiving antenna locations [dB-W/sq m] for at least a fraction q of the time, from (8).
$S_{v,s,g,c,5}$	A Fresnel integral [34, p. III-18], for (92,137,167).
S_V	Scattering volume term [dB] of tropospheric scatter calculations, from (219).
T	A parameter defined and used in (83), the $G_{\frac{F}{h}}$ formulation.
T	Relaxation time [us] used in the calculation of water surface constants, for (151).
Tan-'	Inverse tangent [rad] with principal value.
TWIRL	A program name [20, p. 9].
$T'_{eo,s,w}$	Storm height or layer thickness (Figure 12) used in attenuation calculations for oxygen absorption (T_{eo}), rain storm attenuation (T_{es}), or water vapor absorption (T_{ew}).
UHF	Ultra-High Frequency [300 to 3000 MHz].
v	Knife-edge diffraction parameter, from (90).
$V_{0,c,5}$	Knife-edge diffraction parameters used to determine $f_{g,c,5}$, from (135,165).
VHF	Very High Frequency [30 to 300 MHz).
V/V	Volts per volt.
V(0.5)	A parameter [dB], from (235,246).
$V_c(q)$	Variability for specific climate or time block, from (265).
$V_e(0.5)$	Variability adjustment term [dB], from (240).
$V_{I,i,FM}$	Variability levels (V_1, . . . V_i, . . . V_M) used in mixing distributions (Sec. 10.6).
W	A weighting factor used in combining knife-edge and rounded earth diffraction attenuations, from (94).
W	Watts.

SHF	Super High Frequency [3 to 30 GHz].
Sin-'	Inverse sine with principal value.
S_e	Scattering efficiency term [dB] used in tropospheric scatter calculations, from (208).
$S_{R(q)}$	Power density at receiving antenna locations [dB-W/sq m] for at least a fraction q of the time, from (8).
$S_{v,s,g,c,5}$	A Fresnel integral [34, p. III-18], for (92,137,167).
S_V	Scattering volume term [dB] of tropospheric scatter calculations, from (219).
T	A parameter defined and used in (83), the $G_{\frac{F}{h}}$ formulation.
T	Relaxation time [us] used in the calculation of water surface constants, for (151).
Tan-'	Inverse tangent [rad] with principal value.
TWIRL	A program name [20, p. 9].
$T'_{eo,s,w}$	Storm height or layer thickness (Figure 12) used in attenuation calculations for oxygen absorption (T_{eo}), rain storm attenuation (T_{es}), or water vapor absorption (T_{ew}).
UHF	Ultra-High Frequency [300 to 3000 MHz].
v	Knife-edge diffraction parameter, from (90).
$V_{0,c,5}$	Knife-edge diffraction parameters used to determine $f_{g,c,5}$, from (135,165).
VHF	Very High Frequency [30 to 300 MHz).
V/V	Volts per volt.
V(0.5)	A parameter [dB], from (235,246).
$V_c(q)$	Variability for specific climate or time block, from (265).
$V_e(0.5)$	Variability adjustment term [dB], from (240).
$V_{I,i,FM}$	Variability levels (V_1, . . . V_i, . . . V_M) used in mixing distributions (Sec. 10.6).
W	A weighting factor used in combining knife-edge and rounded earth diffraction attenuations, from (94).
W	Watts.

$Y_I(q)$ — Variability [dB] associated with ionospheric scintillation, from (263).

$Y_{IC}(q)$ — $Y_I(q)]_C$ for a particular distribution to be used in the mixing process to obtain resultant $Y_I(q)$, from (267).

$Y_r(q)$ — Variability [dB greater than median] associated with rain attenuation, from (261).

$Y_0(0.1)$ or $Y_0(0.9)$ — A reference variability level used to calculate Y(0.1) or Y(0.9), from (235, 246).

Y_{yT} — A top limiting level when the calculations are in the lobing mode in the line-of-sight region, from (241).

Y_{yv} — A parameter from (133).

$Y_{y136}(q)$ — Variability [dB] for (263) that is associated with ionospheric scintillation at 136 MHz [15, p. 45].

$Y_\pi(q)$ — Variability [dB greater than median] of received power used to describe short-term (within-the-hour) fading associated with multipath where q is the faction of time during which a particular level is exceeded (Sec. 10.3).

$Y_\Sigma(q)$ — Total variability [dB greater than median] of received power about its median, $Y_\Sigma(0.5) = 0$, where q is the fraction of time for which a particular value is exceeded, from (229). These values may represent instantaneous levels or hourly median levels depending upon the time availability option selected [20, p. 103, TIME AVAILABILITY OPTIONS].

z — A parameter from (102).

$z_{a1,2}$ — Parameters used in tropospheric scatter calculations, from (186).

$z_{b1,2}$ — Parameters used in tropospheric scatter calculations, from (187).

$z_{z1,2}$ — Parameters [km], from (107).

$Z_{a1,2}$ — Parameters used in tropospheric scatter calculations, from (191).

$Z_{A1,2}$ — Parameters used in tropospheric scatter calculations, from (195).

$Z_{b1,2}$ — Parameters used in tropospheric scatter calculations, from (192).

$Y_I(q)$ Variability [dB] associated with ionospheric scintillation, from (263).

$Y_{IC}(q)$ $Y_I(q)]_C$ for a particular distribution to be used in the mixing process to obtain resultant $Y_I(q)$, from (267).

$Y_r(q)$ Variability [dB greater than median] associated with rain attenuation, from (261).

$Y_0(0.1)$ or $Y_0(0.9)$ A reference variability level used to calculate Y(0.1) or Y(0.9), from (235, 246).

Y_{yT} A top limiting level when the calculations are in the lobing mode in the line-of-sight region, from (241).

Y_{yv} A parameter from (133).

$Y_{136}(q)$ Variability [dB] for (263) that is associated with ionospheric scintillation at 136 MHz [15, p. 45].

$Y_\pi(q)$ Variability [dB greater than median] of received power used to describe short-term (within-the-hour) fading associated with multipath where q is the faction of time during which a particular level is exceeded (Sec. 10.3).

$Y_\Sigma(q)$ Total variability [dB greater than median] of received power about its median, $Y_\Sigma(0.5) = 0$, where q is the fraction of time for which a particular value is exceeded, from (229). These values may represent instantaneous levels or hourly median levels depending upon the time availability option selected [20, p. 103, TIME AVAILABILITY OPTIONS].

z A parameter from (102).

$z_{a1,2}$ Parameters used in tropospheric scatter calculations, from (186).

$z_{b1,2}$ Parameters used in tropospheric scatter calculations, from (187).

$z_{z1,2}$ Parameters [km], from (107).

$Z_{a1,2}$ Parameters used in tropospheric scatter calculations, from (191).

$Z_{A1,2}$ Parameters used in tropospheric scatter calculations, from (195).

$Z_{b1,2}$ Parameters used in tropospheric scatter calculations, from (192).

η	A parameter used in tropospheric scatter calculations, from (211).
θ	Scattering angle [rad] used in tropospheric scatter calculations. It is the angle between transmitter horizon to common volume ray and the common volume to receiver horizon ray as both leave their crossover point, from (197).
$\theta_{al,2}$	Angles [rad], from (178).
$\theta_{Al,2}$	Angles [rad] used in tropospheric scatter calculations; angles between the common volume horizontal and the horizon to the common volume rays as they leave their crossover point, from (196).
θ_{ce}	An angle [rad] shown in Figure 9, from (130).
θ_{eEl}	An initial value for the facility horizon elevation angle [rad] that is based on effective earth radius geometry, and is shown in Figure 4. It may be specified [20, p. 90, HORIZON OBSTACLE ABOVE HORIZONTAL AT FACILITY] or calculated as indicated in Figure 5.
$\theta_{esRl,2}$	Smooth earth horizon ray elevation angle [rad] at the appropriate terminal as determined from ray tracing (Sec. 3.1). Illustrated in Figure 3.
$\theta_{esl,2}$	Final value for smooth earth horizon ray elevation angle [rad] at the appropriate terminal, from (30).
θ_{el}	Elevation angle [rad] of horizon from the facility, from (40).
θ_{e2}	Elevation angle [rad] of aircraft horizon ray shown in Figure 6, from (49).
θ_{e5}	An angle [rad], from (163).
θ_{FL}	Magnitude of earth facility latitude [deg] for (262).
$\theta_{egl,2}$	Elevation angles [rad] of the ground reflected rays at the terminal antennas, from (148).
$\theta_{hl,2}$	Parameter [rad] used to calculate $\theta_{Hl,2}$, from (115).
θ_{h5}	An angle [rad], from (158).
$\theta_{Hl,2}$	Direct ray elevation angles [rad] at the terminal antennas, from (147).

$\theta_{kg,c}$	Angles [rad] used in (135), from (132,134).
θ_{eL}	Elevation angle [rad] of horizon-to-aircraft ray at facility horizon (Figure 4), from (42).
$\theta_{eL1,2}$	Horizon elevation angle [rad] adjustment terms, from (146).
θ_{eO}	Central angle [rad], from (117).
$\theta_{r1,2}$	Angles [rad] used in (148), from (116).
θ_{eS}	An angle [rad], from (180).
$\theta_{sR1,2}$	Smooth earth horizon ray elevation angles [rad] that are obtained using ray tracing horizon distances with an effective earth formulation and shown in Figure 3, from (23).
$\theta_{s1,2}$	Central angles [rad] below the smooth earth terminal to horizon distances, from (29).
θ_{eV}	Diffraction angle [rad] for the O-A path (Figure 7), from (89).
$\theta_{e1,2}$	Angles [rad] shown in Figure 8, from (108).
$\theta_{e3,4}$	Angles [rad], from (57,58).
θ_{e5}	An angle [rad], from (159).
θ_{6}	An angle [rad], from (164).
κ	Wave number [per km], from (214).
λ	Wavelength [km], from (10).
λ_m	Wavelength [m], from (10).
μs	Microseconds [10^{-6} sec].
π	The constant 3.141592654.
$\rho_{1,2}$	Parameters used in tropospheric scatter calculations, from (215).
	Surface conductivity [mho/m], a model input parameter [20, p. 99, SURFACE TYPE OPTIONS].

$\theta_{kg,c}$	Angles [rad] used in (135), from (132,134).
θ_{eL}	Elevation angle [rad] of horizon-to-aircraft ray at facility horizon (Figure 4), from (42).
$\theta_{eL1,2}$	Horizon elevation angle [rad] adjustment terms, from (146).
θ_{eo}	Central angle [rad], from (117).
$\theta_{m1,2}$	Angles [rad] used in (148), from (116).
θ_{es}	An angle [rad], from (180).
$\theta_{sR1,2}$	Smooth earth horizon ray elevation angles [rad] that are obtained using ray tracing horizon distances with an effective earth formulation and shown in Figure 3, from (23).
$\theta_{s1,2}$	Central angles [rad] below the smooth earth terminal to horizon distances, from (29).
θ_v	Diffraction angle [rad] for the O-A path (Figure 7), from (89).
$\theta_{?1,2}$	Angles [rad] shown in Figure 8, from (108).
$\theta_{e3,4}$	Angles [rad], from (57,58).
θ_{e5}	An angle [rad], from (159).
θ_6	An angle [rad], from (164).
K	Wave number [per km], from (214).
λ	Wavelength [km], from (10).
λ_m	Wavelength [m], from (10).
μs	Microseconds [10^{-6} sec].
π	The constant 3.141592654.
$\rho_{?1,2}$	Parameters used in tropospheric scatter calculations, from (215).
	Surface conductivity [mho/m], a model input parameter [20, p. 99, SURFACE TYPE OPTIONS].

REFERENCES

[1] Ames, L. A., P. Newman, and T. F. Rogers (1955), VHF tropospheric overwater measurements far beyond the radio horizon, Proc. IRE 43, No. 10, 1369-1373.

[2] Barnett, W. T. (1972), Multipath propagation at 4, 6, and 11 GHz, Bell Sys. Tech. J. 51, No. 2, 321-361.

[3] Bean, B. R., and E. J. Dutton (1968), Radio Meteorology (Dover Publications, Inc., New York, N.Y.).

[4] Bean, B. R., and G. D. Thayer (1959), CRPL Exponential Reference Atmosphere, NBS Monograph 4 (NTIS, PB-174^987).

[5] Beard, C. I. (1961), Coherent and incoherent scattering of microwaves from the ocean, IRE Trans. Ant. Prop. AP-9, No. 5, 470-483.

[6] Bremmer, H. (1949), Terrestrial Radio Waves (Elsevier Pub. Co., New York, N.Y.).

[7] CCIR (1982), Propagation data required for trans-horizon radio-relay systems, Report 238-4, XVth Plenary Assembly, Geneva (Intl. Telecom. Union, Geneva).

[8] CCIR (1982), VHF, UHF, and SHF propagation curves for the aeronautical mobile service, Rec. 528-2, XVth Plenary Assembly, Geneva (Intl. Telecom. Union, Geneva).

[9] Dougherty, H. T. (1967), Microwave fading with airborne terminals, ESSA Tech. Report IER 58-ITSA 55 (NTIS, N-70-73581).

[10] Gierhart, G. D., A. P. Barsis, M. E. Johnson, E. M. Gray, and F. M. Capps (1971), Analysis of air-ground radio wave propagation measurements at 890 MHz, Office of Telecommunications Report OT/TRER 21 (NTIS, COM-75-10830/AS).

[11] Gierhart, G. D., R. W. Hubbard, and D. V. Glen (1970), Electrospace planning and engineering for the air traffic environment, Department of Transportation Report, FAA-RD-70-71 (NTIS, AD 718 447).

[12] Gierhart, G. D., and M. E. Johnson (1969), Transmission loss atlas for select aeronautical service bands from 0.125 to 15.5 GHz, ESSA Technical Report ERL 111-ITS 79 (GPO, $1.25).

[13] Gierhart, G. D., and M. E. Johnson (1972), UHF transmission loss estimates for GOES, Office of Telecommunications Technical Memo. OT TM-109 (NTIS, COM-73-40339).

[14] Gierhart, G. D., and M. E. Johnson (1973), Computer programs for air/ground propagation and interference analysis, 0.1 to 20 GHz, DOT Report FAA-RD-73-103 (NTIS, AD 770 335).

[15] Gierhart, G. D., and M. E. Johnson (1978), Propagation model (0.1 to 20 GHz) extensions for 1977 computer programs, DOT Report FAA-RD-77-129 (NTIS, ADA 055605).

REFERENCES

[1] Ames, L. A., P. Newman, and T. F. Rogers (1955), VHF tropospheric overwater measurements far beyond the radio horizon, Proc. IRE 43, No. 10, 1369-1373.

[2] Barnett, W. T. (1972), Multipath propagation at 4, 6, and 11 GHz, Bell Sys. Tech. J. 51, No. 2, 321-361.

[3] Bean, B. R., and E. J. Dutton (1968), Radio Meteorology (Dover Publications, Inc., New York, N.Y.).

[4] Bean, B. R., and G. D. Thayer (1959), CRPL Exponential Reference Atmosphere, NBS Monograph 4 (NTIS, PB-174^987).

[5] Beard, C. I. (1961), Coherent and incoherent scattering of microwaves from the ocean, IRE Trans. Ant. Prop. AP-9, No. 5, 470-483.

[6] Bremmer, H. (1949), Terrestrial Radio Waves (Elsevier Pub. Co., New York, N.Y.).

[7] CCIR (1982), Propagation data required for trans-horizon radio-relay systems, Report 238-4, XVth Plenary Assembly, Geneva (Intl. Telecom. Union, Geneva).

[8] CCIR (1982), VHF, UHF, and SHF propagation curves for the aeronautical mobile service, Rec. 528-2, XVth Plenary Assembly, Geneva (Intl. Telecom. Union, Geneva).

[9] Dougherty, H. T. (1967), Microwave fading with airborne terminals, ESSA Tech. Report IER 58-ITSA 55 (NTIS, N-70-73581).

[10] Gierhart, G. D., A. P. Barsis, M. E. Johnson, E. M. Gray, and F. M. Capps (1971), Analysis of air-ground radio wave propagation measurements at 890 MHz, Office of Telecommunications Report OT/TRER 21 (NTIS, COM-75-10830/AS).

[11] Gierhart, G. D., R. W. Hubbard, and D. V. Glen (1970), Electrospace planning and engineering for the air traffic environment, Department of Transportation Report, FAA-RD-70-71 (NTIS, AD 718 447).

[12] Gierhart, G. D., and M. E. Johnson (1969), Transmission loss atlas for select aeronautical service bands from 0.125 to 15.5 GHz, ESSA Technical Report ERL 111-ITS 79 (GPO, $1.25).

[13] Gierhart, G. D., and M. E. Johnson (1972), UHF transmission loss estimates for GOES, Office of Telecommunications Technical Memo. OT TM-109 (NTIS, COM-73-40339).

[14] Gierhart, G. D., and M. E. Johnson (1973), Computer programs for air/ground propagation and interference analysis, 0.1 to 20 GHz, DOT Report FAA-RD-73-103 (NTIS, AD 770 335).

[15] Gierhart, G. D., and M. E. Johnson (1978), Propagation model (0.1 to 20 GHz) extensions for 1977 computer programs, DOT Report FAA-RD-77-129 (NTIS, ADA 055605).

[32] Norton, K. A., L. E. Vogler, W. V. Mansfield, and P. J. Short (1955), The probability distribution of the amplitude of a constant vector plus a Rayleigh-distributed vector, Proc. IRE 43, No. 10, 1354-1361.

[33] Reed, H. R., and C. M. Russell (1964), Ultra High Frequency Propagation (Boston Tech. Publishers, Lexington, Mass.).

[34] Rice, P. L., A. G. Longley, K. A. Norton, and A. P. Barsis (1967), Transmission loss predictions for tropospheric communications circuits, NBS Tech. Note 101, I and II revised (NTIS, AD 687 820 and AD 687 821)[2].

[35] Riblet, H. J., and C. B. Baker (1948), A general divergence formula, J. Appl. Phys. 19, 63-70.

[36] Saxton, J. A., and J. A. Lane (1952), Electrical properties of sea water, Wireless Engr. 29, 6-7.

[37] Thayer, G. D. (1967), A rapid and accurate ray tracing algorithm for a horizontally stratified atmosphere, Radio Sci. 1, (New Series), No. 2, 249-252.

[38] Whitney, H. II., J. Aarons, and R. S. Allen (1972), Estimation of the cumulative amplitude probability distribution function of ionospheric scintillations, Radio Sci. 7, No. 12, 1095-1104.

[39] Whitney, H. E., J. Aarons, and D. R. Seemann (1971), Estimation of the cumulative amplitude probability distribution function of ionospheric scintillations, Air Force Cambridge Res. Labs. Report AFCRL-71-0525, Cambridge, Mass.

[1] Copies of this report were sold for the indicated price by the Superintendent of Documents, U. S. Government Printing Office, Washington, DC 20402, and may still be available.

[2] Copies of these reports are sold by the National Technical Information Services (NTIS), 5285 Port Royal Road, Springfield, VA 22161. Order by indicated accession number.

[3] Copy of this handbook may be ordered from the Commanding Officer, Naval Publications and Forms Center, ATTN: NPFC 3015, 5801 Tabor Avenue, Philadelphia, PA 19120; telephone: 215-697-3321.

[32] Norton, K. A., L. E. Vogler, W. V. Mansfield, and P. J. Short (1955), The probability distribution of the amplitude of a constant vector plus a Rayleigh-distributed vector, Proc. IRE 43, No. 10, 1354-1361.

[33] Reed, H. R., and C. M. Russell (1964), Ultra High Frequency Propagation (Boston Tech. Publishers, Lexington, Mass.).

[34] Rice, P. L., A. G. Longley, K. A. Norton, and A. P. Barsis (1967), Transmission loss predictions for tropospheric communications circuits, NBS Tech. Note 101, I and II revised (NTIS, AD 687 820 and AD 687 821)[2].

[35] Riblet, H. J., and C. B. Baker (1948), A general divergence formula, J. Appl. Phys. 19, 63-70.

[36] Saxton, J. A., and J. A. Lane (1952), Electrical properties of sea water, Wireless Engr. 29, 6-7.

[37] Thayer, G. D. (1967), A rapid and accurate ray tracing algorithm for a horizontally stratified atmosphere, Radio Sci. 1, (New Series), No. 2, 249-252.

[38] Whitney, H. II., J. Aarons, and R. S. Allen (1972), Estimation of the cumulative amplitude probability distribution function of ionospheric scintillations, Radio Sci. 7, No. 12, 1095-1104.

[39] Whitney, H. E., J. Aarons, and D. R. Seemann (1971), Estimation of the cumulative amplitude probability distribution function of ionospheric scintillations, Air Force Cambridge Res. Labs. Report AFCRL-71-0525, Cambridge, Mass.

[1] Copies of this report were sold for the indicated price by the Superintendent of Documents, U. S. Government Printing Office, Washington, DC 20402, and may still be available.

[2] Copies of these reports are sold by the National Technical Information Services (NTIS), 5285 Port Royal Road, Springfield, VA 22161. Order by indicated accession number.

[3] Copy of this handbook may be ordered from the Commanding Officer, Naval Publications and Forms Center, ATTN: NPFC 3015, 5801 Tabor Avenue, Philadelphia, PA 19120; telephone: 215-697-3321.

DOT/FAA/ES-83/3

Systems Engineering
Service
Washington, DC. 20591

The IF-77 Electromagnetic Wave Propagation Model

G. D. Gierhart
and
M. E. Johnson
U.S. Department of Commerce
National Telecommunications and Information Administration
Institute for Telecommunications
Boulder, Colorado 80303

September 1983

Final Report

This document is available to the U.S. public through the National Technical Information Service, Springfield, Virginia 22161.

U.S. Department of Transportation
Federal Aviation Administration